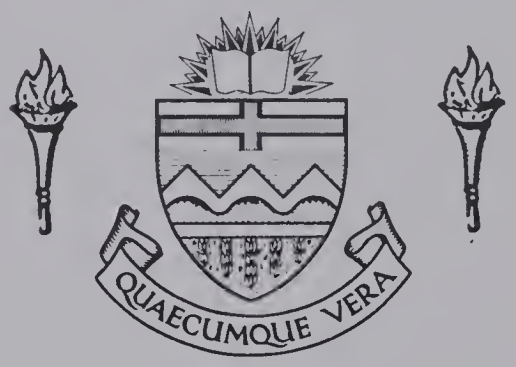

THE UNIVERSITY OF ALBERTA

ASYMMETRIC ICE FORMATION IN CONVECTIVELY COOLED PIPES

by

© ROBERT H. NYREN, B.Sc. (ALBERTA)

A THESIS

SUBMITTED TO THE FACULTY OF GRADUATE STUDIES

IN PARTIAL FULFILLMENT OF THE REQUIREMENTS FOR THE DEGREE

OF MASTER OF SCIENCE

DEPARTMENT OF MECHANICAL ENGINEERING

EDMONTON, ALBERTA

SPRING, 1971

UNIVERSITY OF ALBERTA

FACULTY OF GRADUATE STUDIES

The undersigned certify that they have read, and recommend to the Faculty of Graduate Studies for acceptance, a thesis entitled "ASYMMETRIC ICE FORMATION IN CONVECTIVELY COOLED PIPES" submitted by ROBERT H. NYREN in partial fulfillment of the requirements for the degree of Master of Science.

ABSTRACT

A theoretical analysis is presented for the problem of the transient growth of the ice shell that forms when water, initially at the freezing temperature, flows through a pipe which is convectively cooled to a temperature below the freezing temperature. A solution is sought as a perturbation expansion about the quasi-steady state solution. The first order closed form solutions are found which reveal the influence of external convection and of sensible heat in the ice. The influence of non-uniform convection on the interface shape is displayed graphically for two representative cases and the resulting effect on the pressure gradient is calculated by means of an auxiliary analysis.

Experimental results are presented for the case of superheated water flowing through a uniformly cooled pipe which is inclined. The results for the limiting case of zero superheat agree well with previously obtained results.

ACKNOWLEDGEMENTS

The author wishes to thank the following for their contributions.

- Dr. G.S.H. Lock for supervising this thesis,
- Members of the Mechanical Engineering Shop (particularly Mr. A. Haliburton and Mr. T. Simpson) who aided in construction and modification of experimental apparatus,
- Mrs. L. Moser for typing this thesis,
- The National Research Council for the funds made available under Grant No. A-1672.
- my wife, Brenda for her support.

TABLE OF CONTENTS

LIST OF ILLUSTRATIONS

NOMENCLATURE

T, ϕ	temperature
U, u	axial fluid velocity
P, p	pressure
R, r	radial displacement
A, a	radial displacement of interface
Θ, θ	angular displacement
Z, z	axial displacement
t, τ	time
γ	inclination from horizontal
S	area
w	tube wall thickness
k	thermal conductivity
ρ	density
μ	kinetic viscosity
L	latent heat
Cp	specific heat
κ	thermal diffusivity $[k/\rho Cp]$
h	heat transfer coefficient in coolant
Ste	Stefan number $[Cp(T_f - T_c)/L]$
Bi	Biot number $[hR_1/k]$
α	$Ste_i\ Bi_i/(1 + Bi_i)$
Re	Reynolds number $[U_{AV}\ \rho\ R_1/\mu]$
Pr	Prandtl number
E	flux ratio

σ superheat ratio $[\frac{T_0 - T_f}{T_f - T_c}]$

SUBSCRIPTS

1	tube surface inside, first order
0	tube centerline, zeroth order
c	coolant
f	ice-water interface
w	water
i	ice
ni	ice-free
s	characteristic scale
m	wall
AV	average
o	tube inlet
*	fictitious surface

SUPERSCRIPTS

^	circumferential average

CHAPTER I

INTRODUCTION

The phenomena of solidification and melting are seen in many processes ranging from the natural formation of ice on lakes and rivers to the casting of metals. An understanding of these phenomena is important to the engineer, especially in Canada, where development of northern regions is assuming major proportions.

One problem particularly worthy of attention is the transient solidification of a liquid flowing through a tube, the wall temperature of which is below the solidification temperature of the liquid. As the liquid undergoes a change to the solid phase, thermal energy is released at the moving liquid-solid interface and must be removed by conduction through the solid phase. In addition, some heat may be removed from the flowing liquid.

This type of problem arises in many common situations: for example, a pipeline buried in a region of permafrost, or a water main exposed to a "cold" meteorological environment. A less common situation would be that of hydraulic lines in a space craft which may be subjected to extreme environmental conditions.

As early as 1916 Brush [1] discussed the principles governing the freezing of water in mains. Although he presented no theoretical or experimental results he suggested that the formation of ice in water mains is dependent upon the temperature of the water and its flow rate as well as on the wall temperature.

In 1939 Pekeris and Slichter [2] considered ice formation on the

outside of a long pipe. Their work employed a series expansion in which the zeroth order solution corresponds to the complete neglect of sensible heat in the ice. Higher order terms incorporated the sensible heat which was assumed to be a small fraction of the latent heat.

London and Seban [3] developed a general approximate method for the solution of one dimensional freezing problems for several geometries including freezing in cylinders. Neglecting sensible heat effects in the ice, they used thermal circuitry to develop closed-form solutions for both first and third kind boundary conditions.

Kreith and Romie [4] presented solutions for the case where the interface velocity remains constant. They considered convective cooling for cylinders and spheres where the liquid is initially at the fusion temperature.

In 1962 Allen and Severn [5] used relaxation methods for the case of two dimensional ice formation in planar systems and one dimensional freezing in cylinders. They considered first kind boundary conditions with the liquid initially at the freezing temperature.

In the same year Poots [6] applied integral methods, similar to those employed in solution of boundary layer equations, to problems of solidification. The results for the circular cylinder were compared to those of Allen and Severn with satisfactory agreement.

Zerkle and Sunderland [7] considered the problem of superheated water flowing in a horizontal circular tube. Their theoretical analysis considered steady state conditions and neglected the effects of natural convection. Their experimental results showed considerable

deviation from the theoretical predictions due to the effect of natural convection in the experimental system. The work of Des Ruisseaux and Zerkle [8] is an extension of that of Zerkle and Sunderland and is concerned with predicting conditions under which hydraulic systems will freeze shut.

Gort [9] studied the problem of freezing inside a long vertical cylinder with and without a forced internal flow. He presented approximate solutions for arbitrary wall temperatures for the case of a liquid at the fusion temperature. Experimental results were presented for the case of superheated water flowing in a vertical tube.

Özisik and Mulligan [10] presented an analytical investigation of the freezing of a liquid flowing in a circular tube. Constant wall temperature, slug flow velocity profile, and quasi-steady state heat conduction in the solid phase were assumed. The temperature distributions of both phases were found and these solutions were coupled through the heat balance at the interface to give a single ordinary differential equation for the interface location. Thus interface profiles were found as a function of time and axial locations.

Freeborn [11] investigated the problem of superheated water flowing through a convectively cooled vertical cylinder. The analysis was broken into two parts; an ice free zone near the entry where the superheated water undergoes some cooling, and a zone in which an ice shell forms in the cylinder. The method required the solution of the temperature distribution in the liquid and solid phases with the energy balance at the interface providing a differential equation governing the interface location. Experimental results were presented with satisfactory

agreement between theory and experiment.

The purpose of this thesis is to study the problem of asymmetric freezing in convectively-cooled circular tubes under transient conditions.

A theoretical analysis is presented for fully-developed ice formation in which the effect of sensible heat in the ice is incorporated as well as the effect of non-uniform external convection. The effect of asymmetric ice growth on the internal flow is calculated by an auxiliary analysis.

Experimental results are presented for a different asymmetric situation in which superheated water flows through inclined, convectively-cooled cylinders. Axial as well as azimuthal profiles of the interface are presented.

PART I

THEORETICAL ANALYSIS

CHAPTER II

ICE GROWTH ANALYSIS

2.1 Governing Equations

Consider water, at the fusion temperature, flowing through a very long circular tube which is suddenly immersed in a coolant (see fig. 2.1). The differential equation governing conduction in the ice shell that forms in the tube is given by

$$\frac{\partial^2 T}{\partial R^2} + \frac{1}{R}\frac{\partial T}{\partial R} + \frac{1}{R^2}\frac{\partial^2 T}{\partial \Theta^2} + \frac{\partial^2 T}{\partial Z^2} = \frac{1}{\kappa}\frac{\partial T}{\partial t} \quad , \qquad 2.1\text{-}1$$

where $T(Z,R,\Theta,t)$ is subject to the conditions

$$T(Z,R,\Theta,0) = T_f \quad ,$$

$$T(Z,A,\Theta,t) = T_f \quad ,$$

and

$$k_i \frac{\partial T}{\partial R}(Z,R_1,\Theta,t) = -h(T(Z,R_1,\Theta,t) - T_\infty) \quad .$$

We introduce the normalized non-dimensional variables

$$r = R/R_1 \quad ,$$

$$\theta = \Theta/2\pi \quad ,$$

$$\phi = \frac{T - T_f}{T_f - T_\infty} \quad ,$$

$$z = Z/Z_s \quad ,$$

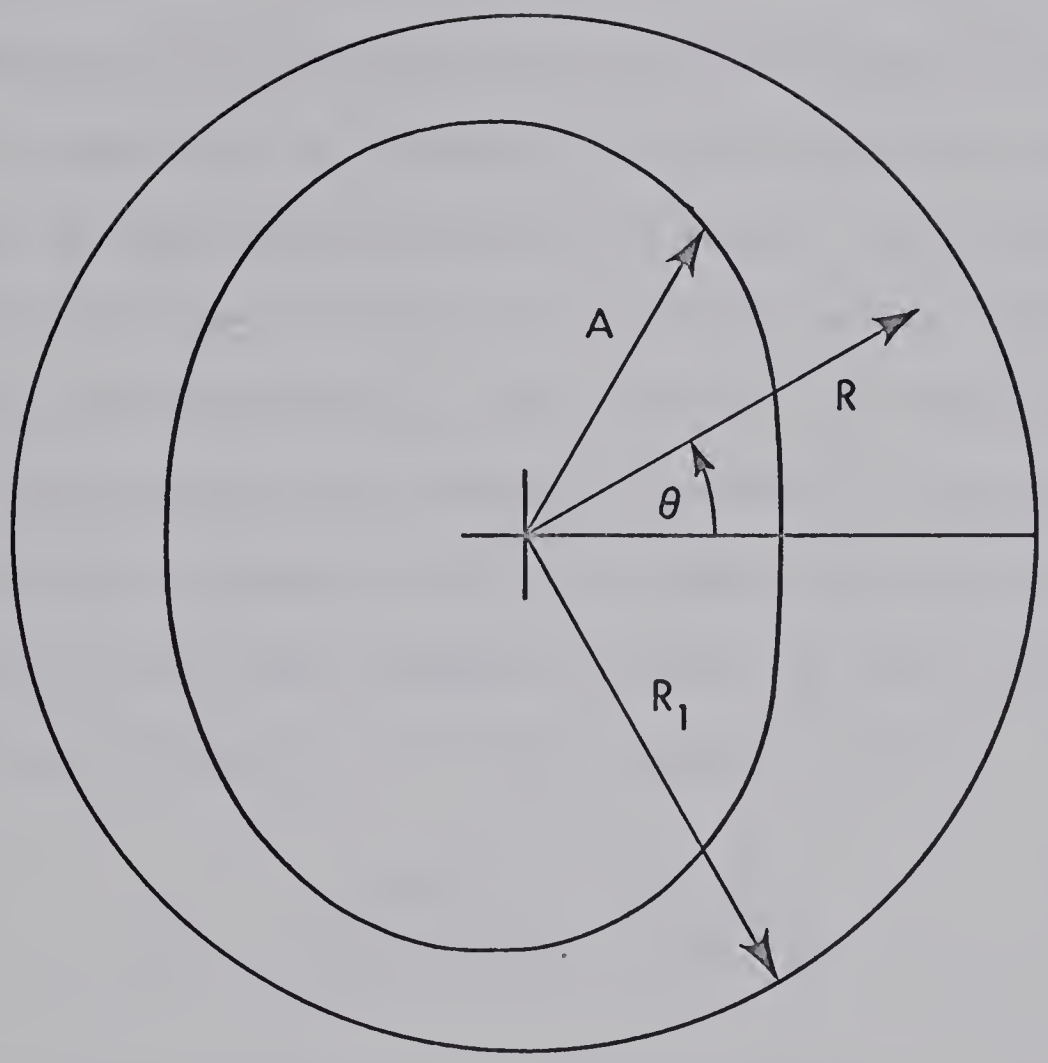

FIG. 2.1: COORDINATE SYSTEM

$$\tau = t/t_s \quad ,$$

and

$$a = A/R_1 \quad ,$$

where Z_s and t_s are length and time scales, respectively. The characteristic length scale for the problem is chosen to be the length of the tube. A characteristic time scale may be found in terms of the other characteristic quantities by estimating the time required to remove the heat released in completely solidifying the water. The time scale thus calculated for the mixed or third kind boundary condition (finite h) is not the same as that found for the Dirichlet or first kind boundary condition. Since the Dirichlet boundary condition is a limiting case ($h \to \infty$) of the mixed boundary condition, a time scale was chosen that is characteristic of a mixed boundary condition for small h but for very large h is characteristic of a Dirichlet boundary condition. Thus we take

$$t_s = \frac{\rho_i L R_1^2}{k_i(T_f - T_\infty)} \cdot \frac{1 + Bi_i}{Bi_i} \quad .$$

Substituting the normalized variables in equation 2.1-1 gives

$$\frac{\partial^2\phi}{\partial r^2} + \frac{1}{r}\frac{\partial\phi}{\partial r} + \left[\frac{1}{4\pi^2}\right]\frac{1}{r^2}\frac{\partial^2\phi}{\partial\theta^2} + \left[\frac{R_1^2}{Z_s^2}\right]\frac{\partial^2\phi}{\partial z^2} = \alpha\frac{\partial\phi}{\partial\tau}$$

where $\alpha = \dfrac{Ste_i\ Bi_i}{1 + Bi_i}$. This simplifies by virtue of the fact that $4\pi^2 >> 1$ and, for a very long tube, $Z_s >> R_1$; and therefore, provided r is not too close to zero it follows that

$$\frac{\partial^2\phi}{\partial r^2} + \frac{1}{r}\frac{\partial\phi}{\partial r} = \alpha\frac{\partial\phi}{\partial\tau} \qquad 2.1\text{-}2$$

offers a good approximation to the description of conduction in the ice. The normalized initial and boundary conditions are then:

$$\phi(r, 0, \alpha) = 0$$

$$\phi(a, \tau, \alpha) = 0 \qquad 2.1\text{-}3$$

$$\text{and} \qquad \frac{\partial \phi}{\partial r}(1, \tau, \alpha) = -Bi_i \left[1 + \phi(1, \tau, \alpha)\right] \ .$$

For this radially symmetric, fully developed, situation the rate at which heat is released per unit length by the moving ice-water interface is equal to $-L\rho_i \, 2\pi \, A \, \frac{dA}{dt}$. Assuming the water remains at the fusion temperature, there will be no heat transferred to or from the water. Therefore, the heat liberated at the interface must be conducted through the ice. Thus, radial interface motion is governed by

$$\rho_i \, L \, \frac{dA}{dt} = k_i \, \frac{\partial T}{\partial R}(A, t) \ .$$

The normalized form of this heat balance equation is

$$\frac{da}{d\tau} = \frac{1 + Bi_i}{Bi_i} \, \frac{\partial \phi}{\partial r}(a, \tau, \alpha) \ , \qquad 2.1\text{-}4$$

the solution of which must satisfy the condition

$$a(0, \alpha) = 1 \qquad 2.1\text{-}5$$

if the system is to be initially ice-free.

2.2 Solution of Equations

In a great many situations $Ste_i \ll 1$ and since α is always less than Ste_i it seems reasonable to seek a solution in the form of a perturbation expansion in powers of α. Thus

$$\phi(r, \tau, \alpha) = \phi_o(r, \tau) + \sum_{n=1}^{\infty} \alpha^n \phi_n (r, \tau) \quad . \qquad 2.2\text{-}1$$

Likewise, a solution to equation 2.1-4 may be sought in the same form: that is

$$a(\tau, \alpha) = a_o(\tau) + \sum_{n=1}^{\infty} \alpha^n a_n(\tau) \quad . \qquad 2.2\text{-}2$$

Substituting 2.2-1 into 2.1-2 and grouping like powers of α we obtain an infinite set of differential equations for the temperature. The first two of these are

$$\frac{\partial^2 \phi_o}{\partial r^2} + \frac{1}{r} \frac{\partial \phi_o}{\partial r} = 0 \qquad 2.2\text{-}3$$

and

$$\frac{\partial^2 \phi_1}{\partial r^2} + \frac{1}{r} \frac{\partial \phi_1}{\partial r} = \frac{\partial \phi_o}{\partial \tau} \qquad 2.2\text{-}4$$

which, to satisfy equations 2.1-3, are subject to the boundary and initial conditions

$$\phi_o(r, 0) = 0$$

$$\phi_o(a_o, \tau) = 0 \qquad 2.2\text{-}5$$

$$\frac{\partial \phi_o}{\partial r} (1, \tau) = -Bi_i \, [1 + \phi_o(1, \tau)]$$

and

$$\phi_1(r, 0) = 0$$

$$\phi_1(a_o, \tau) = -a_1 \frac{\partial \phi_o}{\partial r}(a_o, \tau) \qquad 2.2\text{-}6$$

$$\frac{\partial \phi_1}{\partial r}(1,\tau) = -Bi_i\, \phi_1(1, \tau) \quad .$$

Solutions of equations 2.2-3 and 2.2-4 which satisfy the above conditions are:

$$\phi_o(r, \tau) = -F_o(\tau) \ln \frac{r}{a_o} \qquad 2.2\text{-}7$$

$$\phi_1(r, \tau) = F_1(\tau)\left[r^2 \ln \frac{r}{a_o} - r^2 \left(\frac{F_o + 1}{F_o}\right)\right] + F_2(\tau) \ln r + F_3(\tau) \qquad 2.2\text{-}8$$

where

$$F_o(\tau) = \frac{Bi_i}{1 - Bi_i \ln a_o} \quad ,$$

$$F_1(\tau) = -\frac{da_o}{d\tau} \frac{F_o^2 a_o}{4} \quad ,$$

$$F_2(\tau) = \frac{F_1}{a_o^2}\left[1 + \frac{2}{Bi_i}\left(1 + \frac{1}{Bi_i}\right)\right] - F_1(1 + F_o) - \frac{F_o^2 a_1}{a_o} \quad ,$$

and

$$F_3(\tau) = -\frac{F_2}{Bi_i} + \frac{F_1}{a_o^2}\left[1 + \frac{2}{Bi_i}\left(1 + \frac{1}{Bi_i}\right)\right] \quad .$$

The solutions 2.2-7 and 2.2-8 are incomplete because they contain the time-dependent functions a_o and a_1 which are unknown. However, these functions may be found by substituting equations 2.2-1 and 2.2-2 into

2.1-4 and collecting like powers of α. The first two of the resulting infinite set of differential equations are

$$\frac{da_o}{d\tau} = \frac{1 + Bi_i}{Bi_i} \frac{\partial \phi_o}{\partial r} (a_o, \tau) \qquad 2.2\text{-}9$$

and $$\frac{da_1}{d\tau} = \frac{1 + Bi_i}{Bi_i} \left[\frac{\partial \phi_1}{\partial r} (a_o, \tau) + a_1 \frac{\partial^2 \phi_o}{\partial r^2} (a_o, \tau)\right] \qquad 2.2\text{-}10$$

with the associated initial conditions (from equation 2.1-5)

$$a_o(0) = 1$$

and $$a_1(0) = 0 \; . \qquad 2.2\text{-}11$$

Equations 2.2-7 and 2.2-9 combine to give

$$\frac{da_o}{d\tau} = - \frac{1 + Bi_i}{Bi_i} \cdot \frac{F_o}{a_o} \qquad 2.2\text{-}12$$

$$\text{or} \quad d\tau = - \frac{Bi_i}{1 + Bi_i} \frac{a_o}{F_o} da_o$$

which integrates subject to 2.2-11 to give

$$\tau = \frac{Bi_i}{1 + Bi_i} \left\{\frac{a_o^2 \ln a_o}{2} + (1 - a_o^2) \frac{Bi_i + 2}{4Bi_i}\right\} \; . \qquad 2.2\text{-}13$$

Now using equations 2.2-7 and 2.2-8 in equation 2.2-10 gives

$$\frac{da_1}{d\tau} = \frac{1 + Bi_i}{Bi_i} \{\frac{da_o}{d\tau} [\frac{F_o^2}{4} (1 + \frac{2}{F_o}) + \frac{F_o^2}{4} (1 + F_o) - \frac{F_o^3}{4a_o^2} (1 + \frac{2}{Bi_i} (1 + \frac{1}{Bi_i}))]$$

$$- \frac{F_o^2 a_1}{a_o^2} + \frac{a_1 F_o}{a_o^2}\} \quad .$$

Rearranging

$$\frac{da_1}{da_o} + a_1 [\frac{1 + Bi_i}{Bi_i} (\frac{F_o^2}{a_o^2} - \frac{F_o}{a_o^2})/(\frac{da_o}{d\tau})] = \frac{1 + Bi_i}{Bi_i} [\frac{F_o}{2} + \frac{F_o^2}{4} + \frac{F_o^3}{4}$$

$$- \frac{F_o^3}{4a_o^2} (1 + \frac{2}{Bi_i} (1 + \frac{1}{Bi_i}))] \quad .$$

Substituting for $\frac{da_o}{d\tau}$ from equation 2.2-12 this becomes

$$\frac{da_1}{da_o} + (\frac{1 - F_o}{a_o}) a_1 = \frac{1 + Bi_i}{Bi_i} [\frac{F_o}{2} + \frac{F_o^2}{4} + \frac{F_o^3}{4} - \frac{F_o^3}{4a_o^2} (1 + \frac{2}{Bi_i} (1 + \frac{1}{Bi_i}))] \quad .$$

2.2-14

Formal integration of equation 2.2-14 subject to 2.2-11 then gives

$$a_1 = \frac{1 + Bi_i}{Bi_i} e^{-\int \frac{1 - F_o}{a_o} da_o} \int [\frac{F_o}{2} + \frac{F_o^2}{4} + \frac{F_o^3}{4} - \frac{F_o^3}{4a_o^2} (1 + \frac{2}{Bi_i} (1 + \frac{1}{Bi_i}))]$$

$$e^{\int \frac{1 - F_o}{a_o} da_o} da_o$$

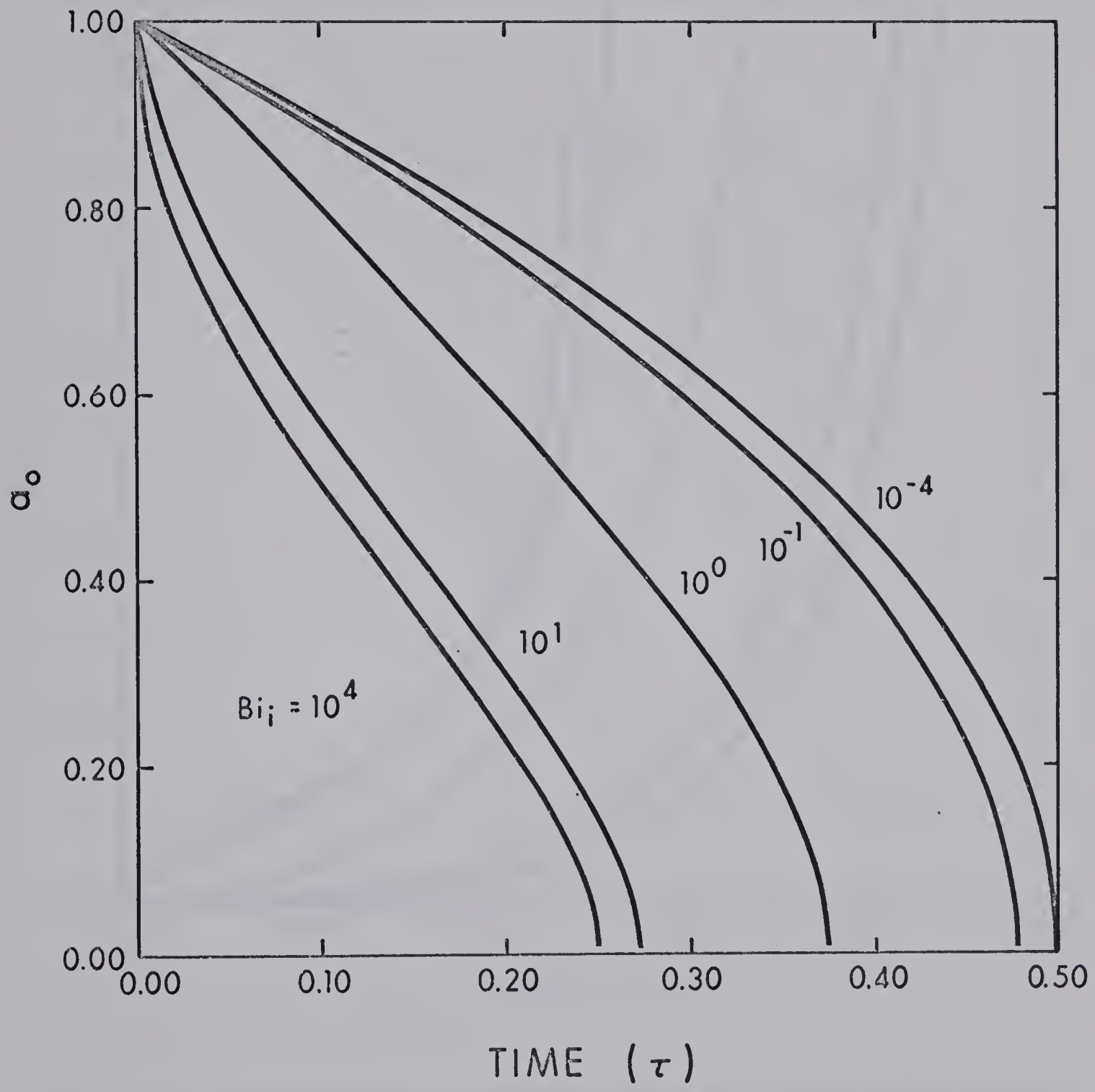

FIG. 2.2: ZEROTH-ORDER SOLUTION FOR INTERFACE GROWTH

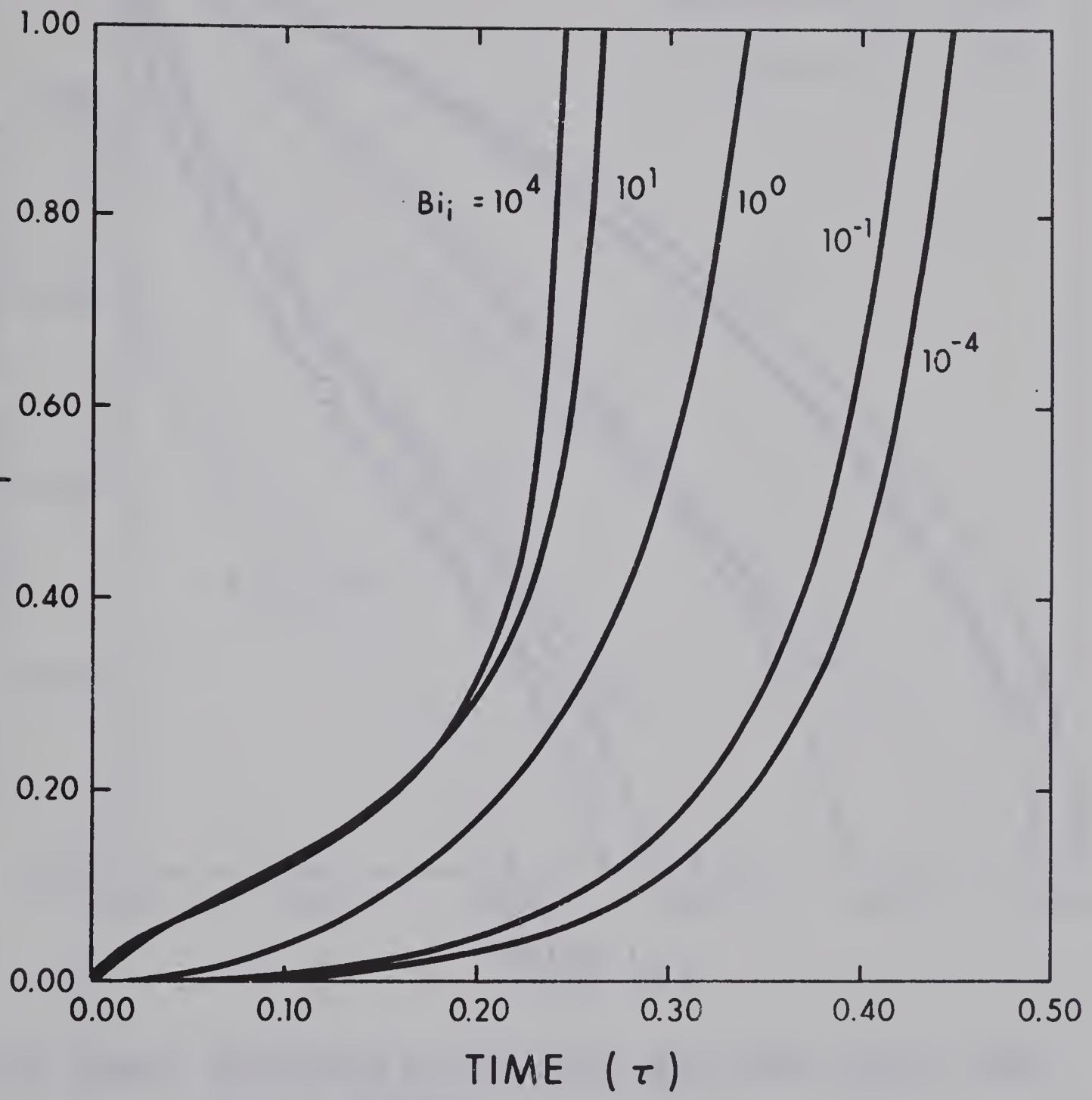

FIG. 2.3: FIRST ORDER CONTRIBUTION TO INTERFACE GROWTH

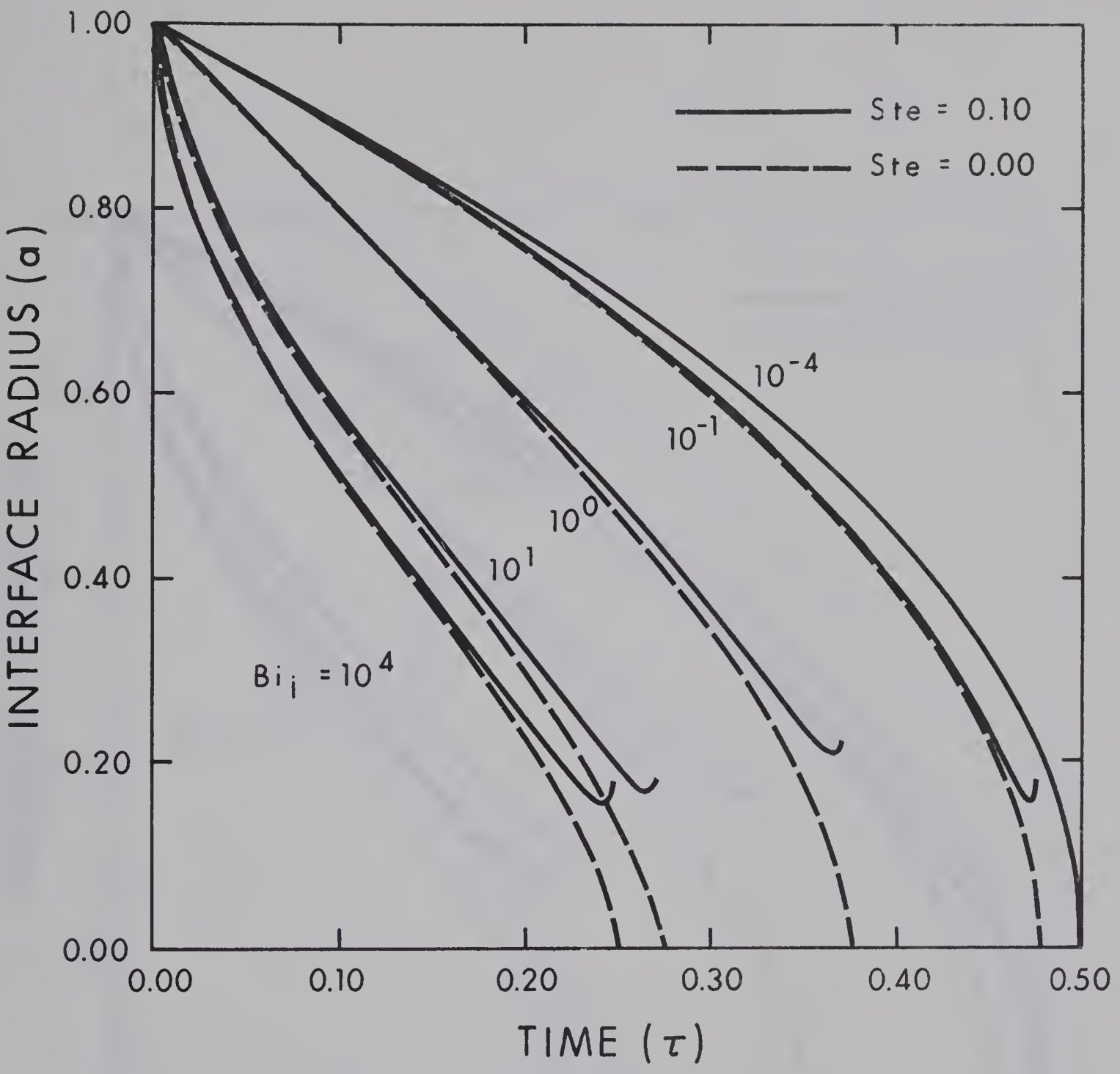

FIG. 2.4(a): THE EFFECT OF SENSIBLE HEAT AND CONVECTION ON ICE GROWTH

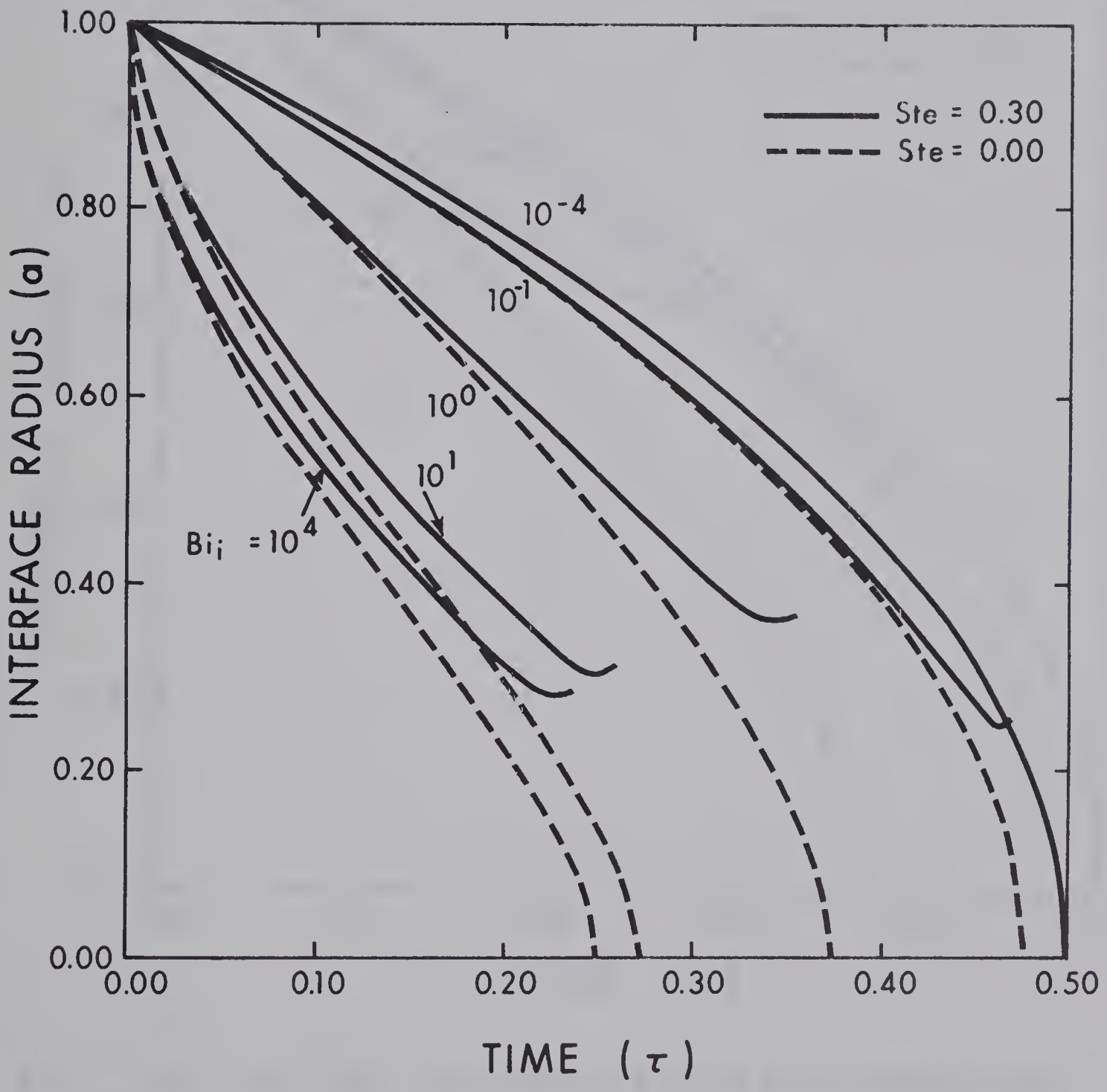

FIG. 2.4(b): THE EFFECT OF SENSIBLE HEAT AND CONVECTION ON ICE GROWTH

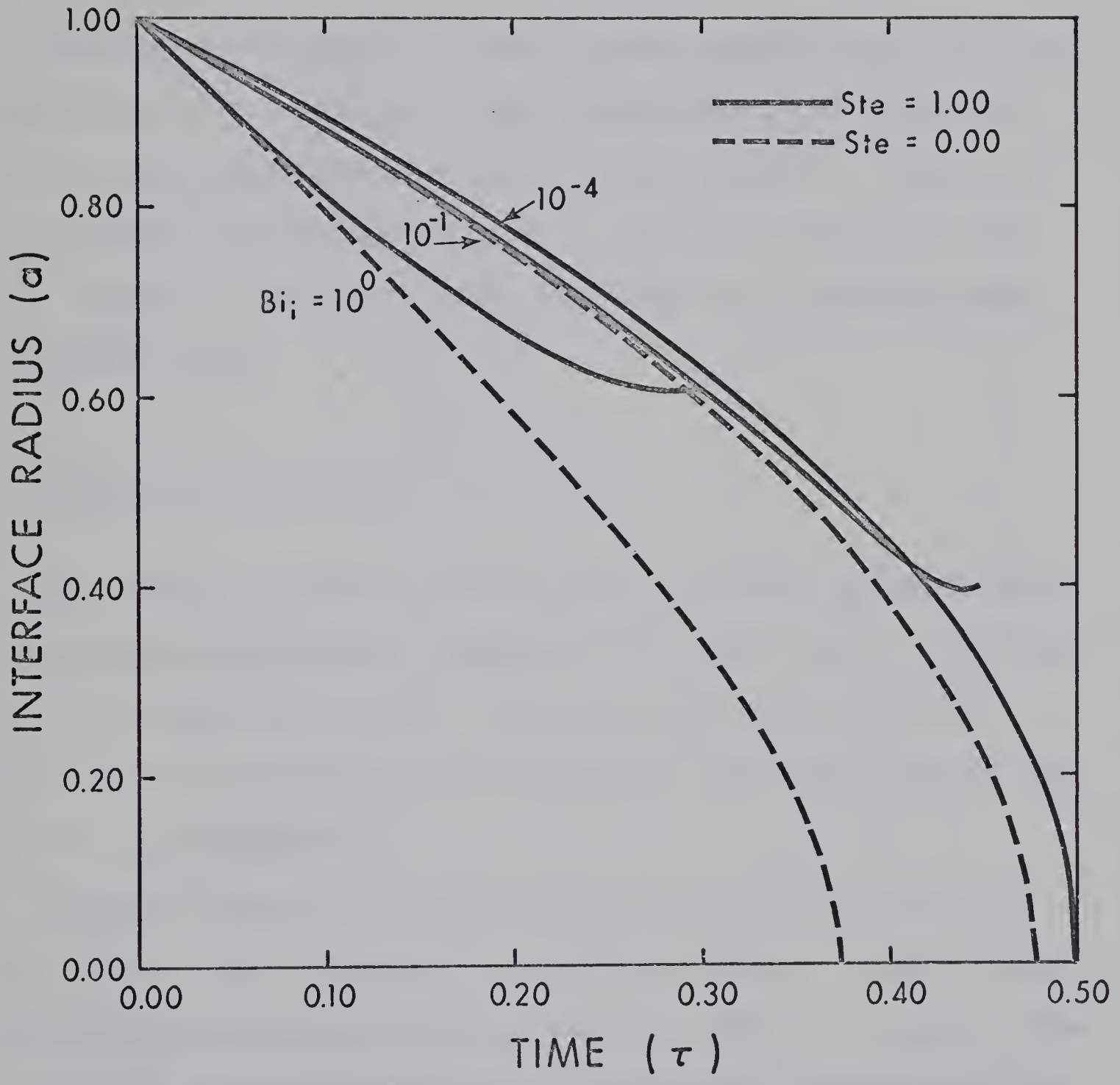

FIG. 2.4(c): THE EFFECT OF SENSIBLE HEAT AND CONVECTION ON ICE GROWTH

or

$$a_1 = \frac{1 + Bi_i}{Bi_i} \frac{F_o}{a_o} \left[\frac{a_o^2 - 1}{4} (1 + F_o) - \frac{F_o - Bi_i}{2Bi_i} (1 + \frac{1}{Bi_i})\right] . \quad 2.2\text{-}15$$

Equations 2.2-13 and 2.2-15 may be used to express as functions of time both a_o and a_1; and, for a given Stefan number, the first order (i.e. $a_o + \alpha a_1$) approximation to the interface location. Figures 2.2 and 2.3 reveal the time dependency of a_o and a_1 for various Biot numbers. Figure 2.4 reveals the effect of Stefan number and Biot number on interface growth.

2.3 Non-Uniform Convection

The results of section 2.2 may be used to predict interface shapes generated by circumferential variations in the heat transfer coefficient i.e., in the local Biot number. The results will have validity as long as a close approximation to axi-symmetric conditions exist in the ice shell (see Appendix A).

Figures 2.5 and 2.6 represent changes in the interface size and shape for two cases of asymmetric convective cooling. The Biot number variations were obtained from established data [12] for transverse flow over an isothermal cylinder at various values of the external Reynolds number.

During the growth of the ice shell any water flowing in the tube must experience an increased resistance to flow, due to the reduced cross-sectional area of the liquid region. This poses the question of how interface growth changes the pressure drop.

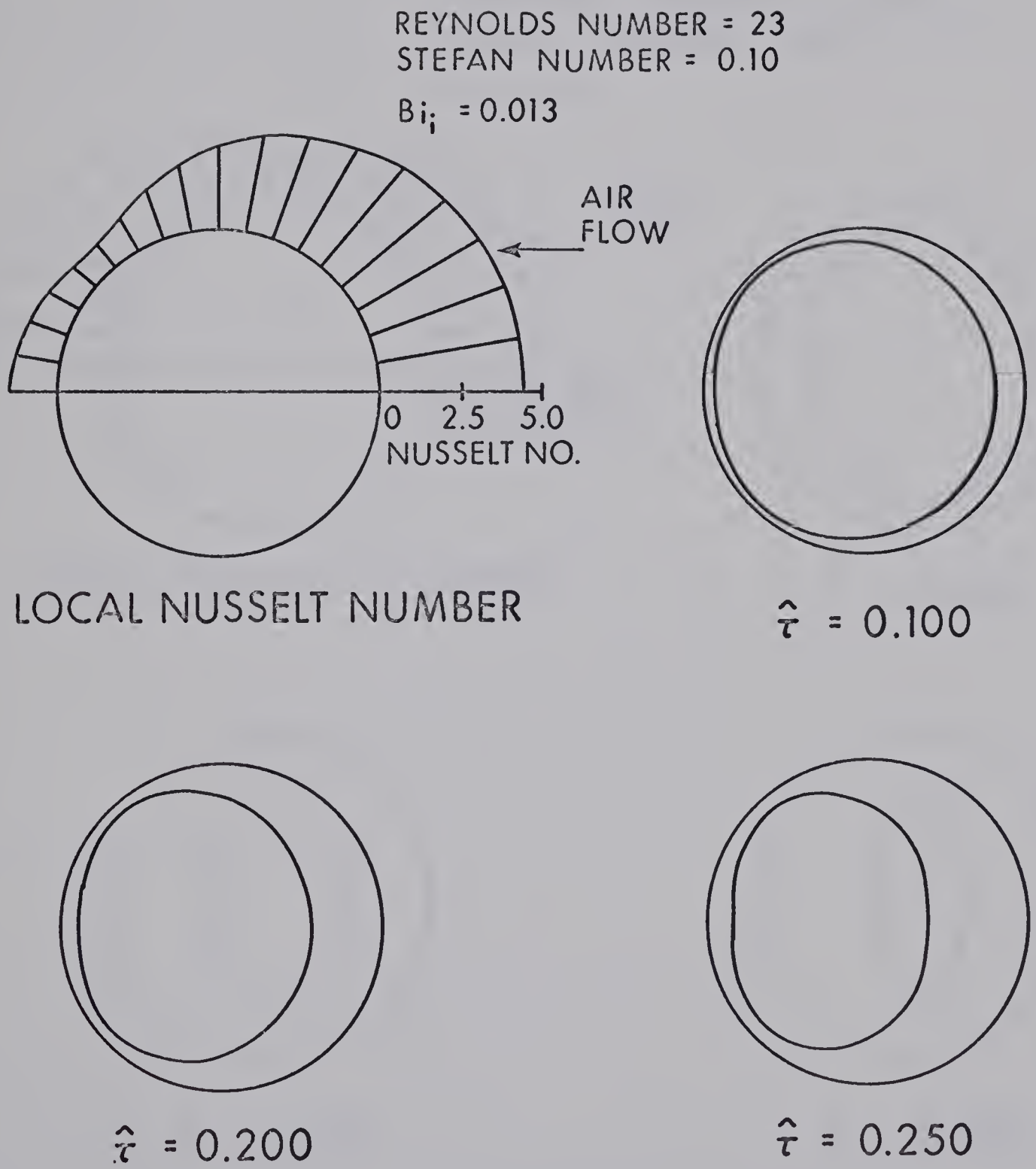

FIG. 2.5: ICE GROWTH IN A TRANSVERSE AIR FLOW: R_E = 23

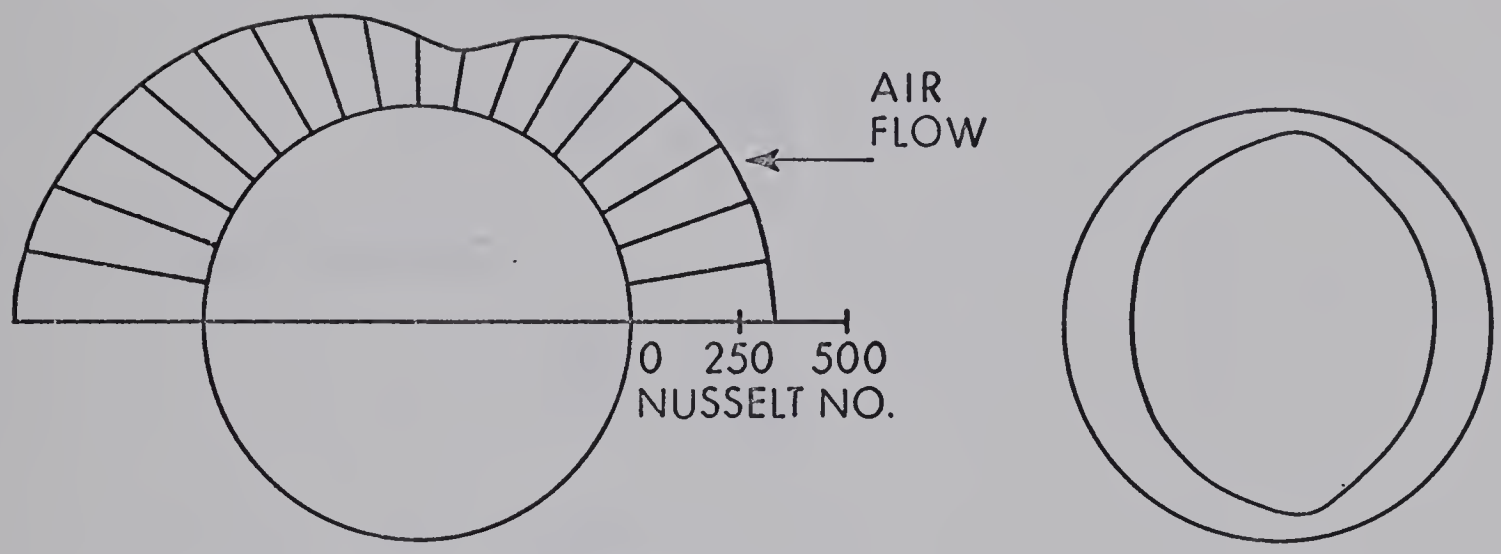

FIG. 2.6: ICE GROWTH IN A TRANSVERSE AIR FLOW: $R_E = 11 \times 10^4$

CHAPTER III

PRESSURE DROP ANALYSIS

3.1 Governing Equations

The fluid velocity is governed by the momentum equation assuming fully developed flow. That is

$$\frac{\partial U}{\partial R^2} + \frac{1}{R}\frac{\partial U}{\partial R} + \frac{1}{R^2}\frac{\partial U}{\partial \Theta} = \frac{\partial P}{\partial X} \quad .$$

Introducing the variables

$$u = U \Big/ \frac{R_*^2}{4\mu} \left(\frac{\partial P}{\partial X}\right)_{ni} \quad ,$$

$$\theta = \Theta/2\pi \quad ,$$

$$r_* = R/R_* \quad ,$$

and

$$\frac{\partial p}{\partial x} = \frac{\partial P}{\partial X} \Big/ \left(\frac{\partial P}{\partial X}\right)_{ni} \quad ,$$

the equation may be written

$$\frac{4\partial p}{\partial x} = \frac{\partial^2 u}{\partial r_*^2} + \frac{1}{r_*}\frac{\partial u}{\partial r_*} + \frac{1}{4\pi^2 r_*^2}\frac{\partial^2 u}{\partial \theta^2} \quad . \qquad 3.1\text{-}1$$

It is clear from figures 2.5 and 2.6 that the interface does not generally possess a regular shape and therefore it is necessary to solve equation 3.1-1 within arbitrarily shaped boundaries. There are several available techniques [13, 14, 15] for such problems. Sparrow and Haji-Sheikh use sophisticated but cumbersome orthonormalizations to

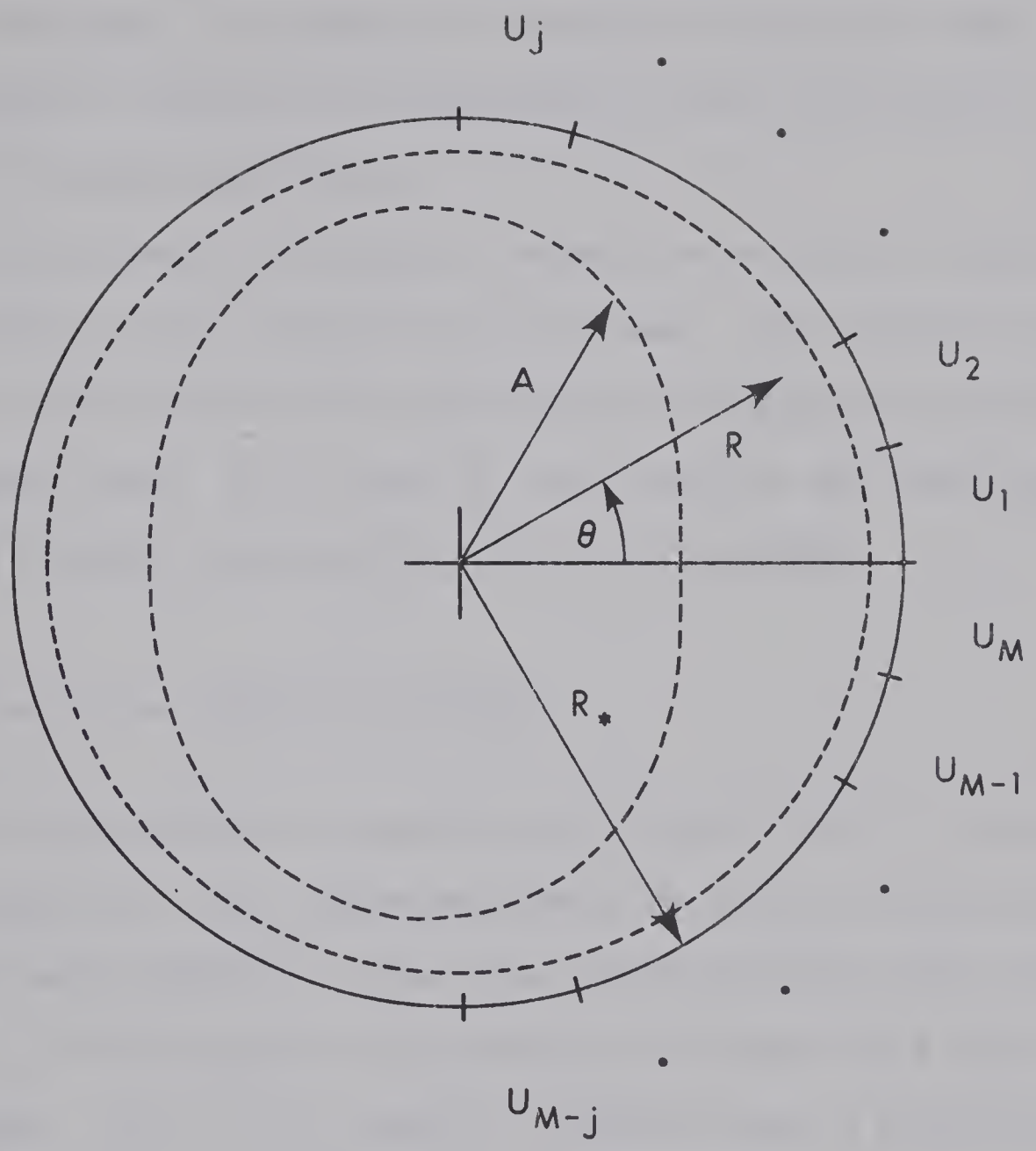

FIG. 3.1: IMBEDDING

give solutions for arbitrary shapes. Tao uses conformal mapping to permit solutions for any shapes for which suitable mappings can be found. In view of the difficulties and limitations involved in these and other techniques it is proposed to develop an alternative semi-analytic method*, similar to that employed by Boley [14], which has the merit of relative simplicity.

This method treats the region of interest as an interior part of a larger region of any convenient size and shape. The solution to equation 3.1-1 is then found for the larger region and adjusted through the outer boundary values, until values at the surface of the inner region satisfy the boundary conditions for the original problem.

3.2 Solution by the Imbedding Technique

Consider the solution of equation 3.1-1 in the interior region shown in figure 3.1. This region represents the area available for liquid flow and is imbedded in the larger region bounded by the circle of radius R_*. This circular outer boundary is divided into a number of equal segments. The j^{th} arc segment is assumed to have a velocity U_j, the magnitude and sign of which is to be determined.

The velocity distribution resulting solely from the movement of one arc is readily found, and by superposition it is found that for m equally wide segments the velocity field is given by

$$u(r_*, \theta) = -\frac{\partial p}{\partial x}(1 - r_*^2) - \sum_{j=1}^{m} u_j f_j (r_*, \theta) \qquad 3.2\text{-}1$$

---

* Analytic in formulation but numerical in execution.

where

$$f_j(r_*, \theta) = \frac{1}{m} + 2 \sum_{n=1}^{\infty} \frac{r_*^{\,n} \sin\left(\frac{\pi n}{m}\right)}{\pi n} \cos n\left(2\pi\,\theta - \left(j - \frac{1}{2}\right)\frac{2\pi}{m}\right) \quad .$$

It now remains to choose the U_j such that the velocity at the ice-water interface is zero. Thus, for any co-ordinate point (a_{*k}, θ_k) on the interface

$$\sum_{j=1}^{m} u_j\, f_j\,(a_{*k}, \theta_k) = -\frac{\partial p}{\partial x}\left(1 - a_{*k}^{\,2}\right) \quad . \qquad 3.2\text{-}2$$

It is evident that a set of m such points on the interface will yield a set of m linear algebraic equations relating the arc velocities U_j to any given set of interface radii. The equations may be solved readily to determine a set of U_j which will produce a zero-velocity contour passing through the chosen co-ordinate points.

As written, equation 3.2-2 cannot be solved unless the pressure gradient is specified. To circumvent this difficulty we define

$$G(r_*, \theta) = -u(r_*, \theta)/\frac{\partial p}{\partial x}$$

thus permitting the calculation of $U_j/\frac{\partial p}{\partial x}$ instead of U_j. The variation of $\frac{\partial p}{\partial x}$ may now be found from the volumetric flow rate given by

$$\dot{Q} = \int U dS$$

$$= -\frac{R_*^{\,2}}{4\pi}\left(\frac{\partial p}{\partial X}\right) \int G(r_*, \theta)\, dS \quad .$$

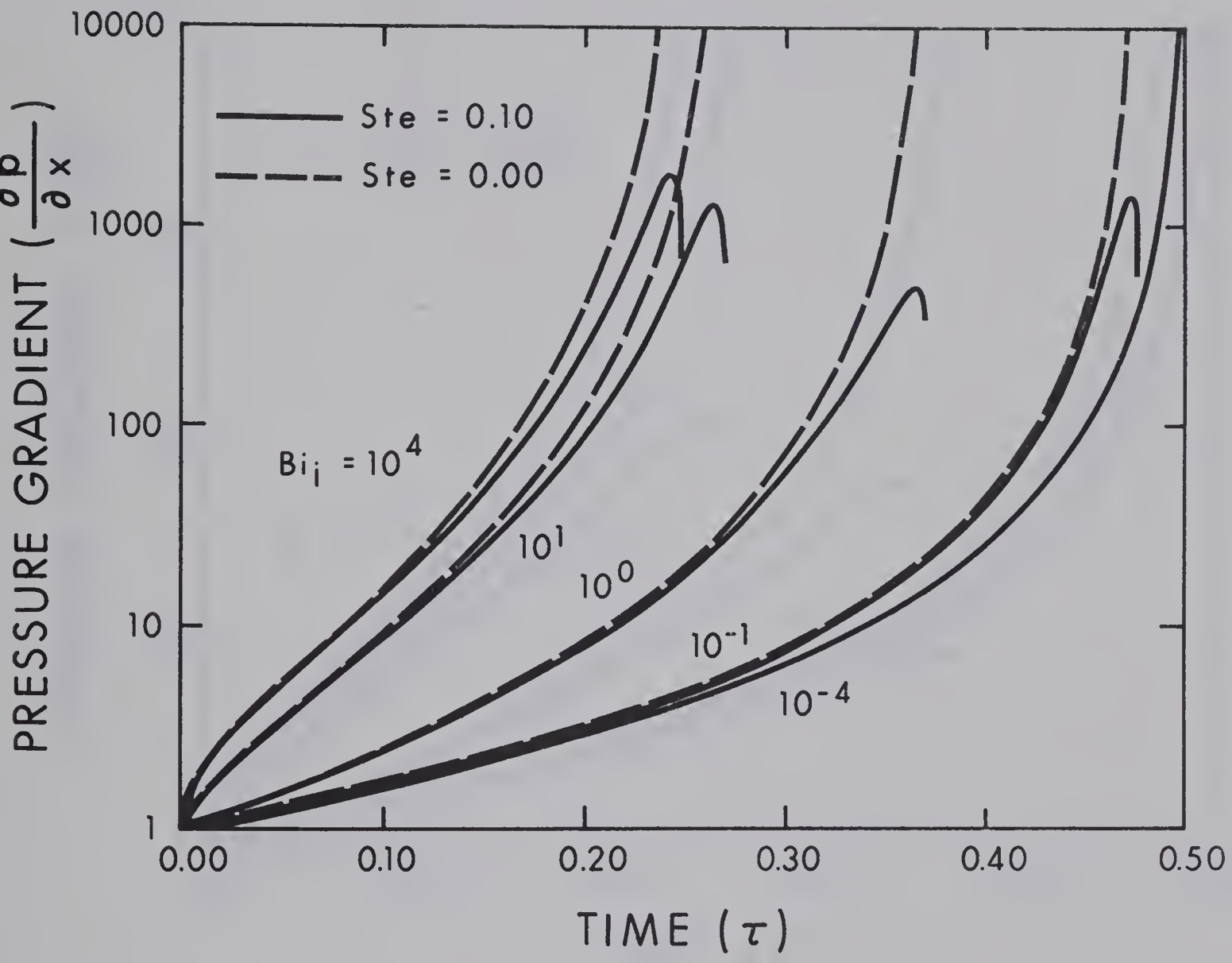

FIG. 3.2(a): EFFECT OF SENSIBLE HEAT AND CONVECTION ON PRESSURE GRADIENT

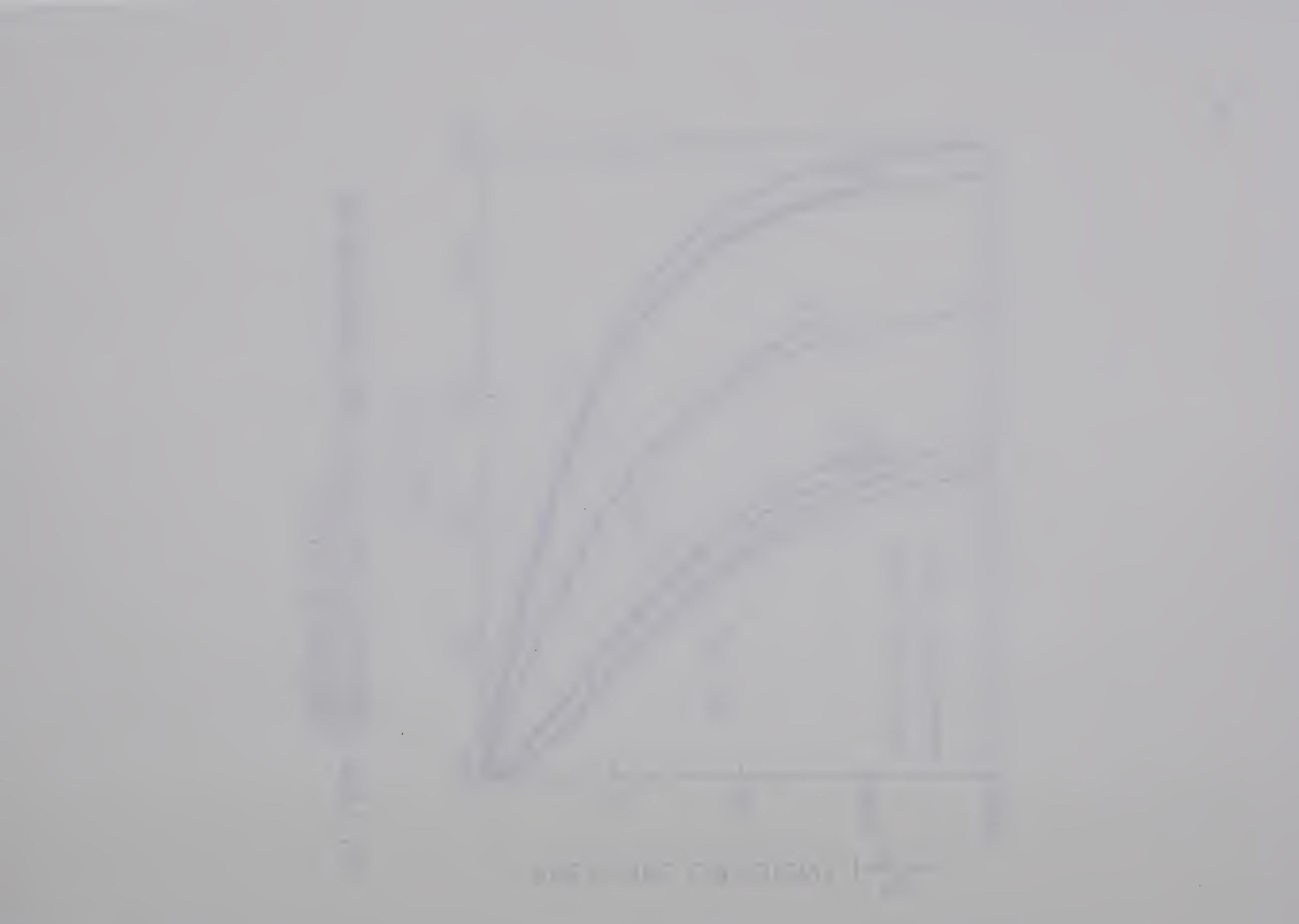

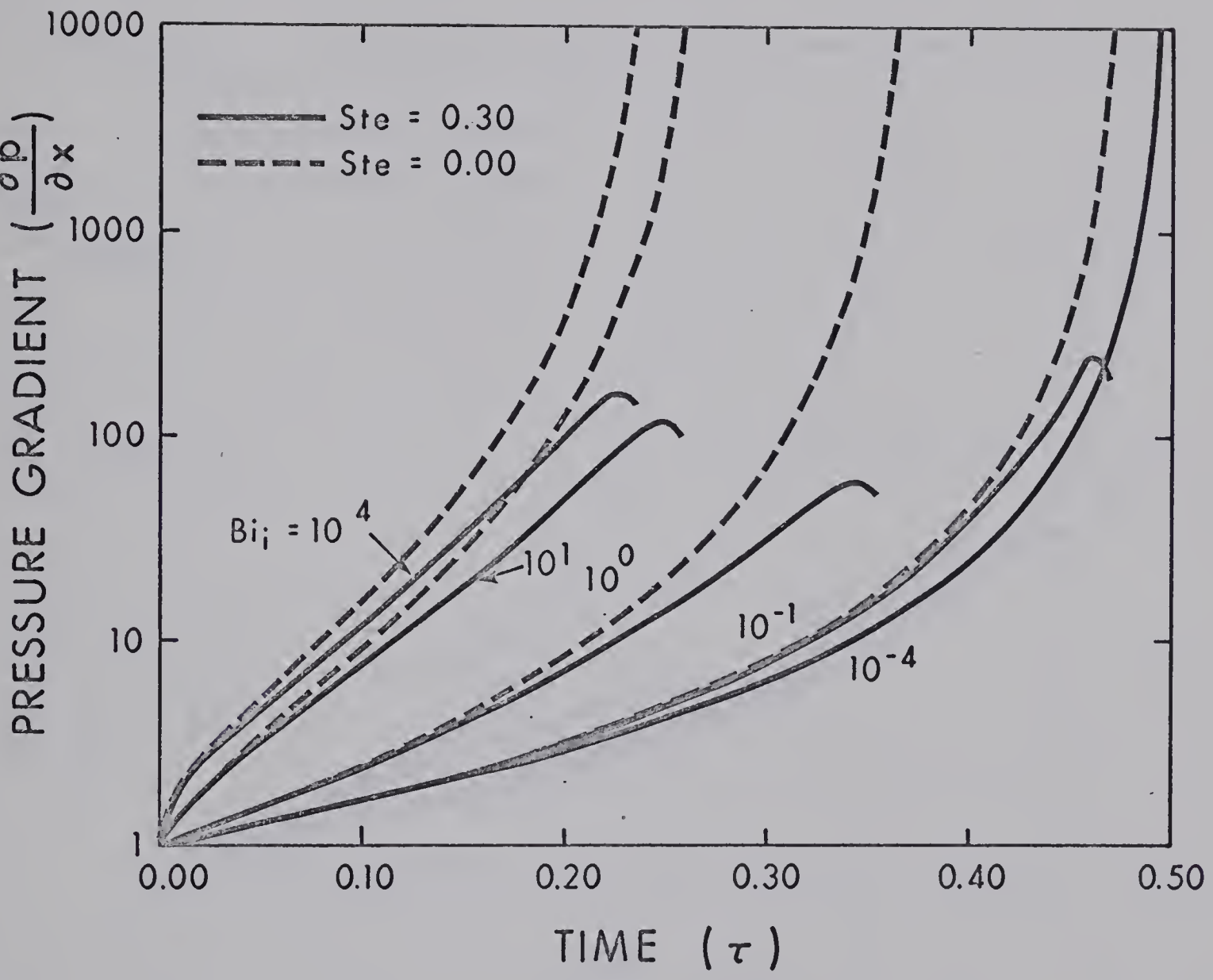

FIG. 3.2(b): EFFECT OF SENSIBLE HEAT AND CONVECTION ON PRESSURE GRADIENT

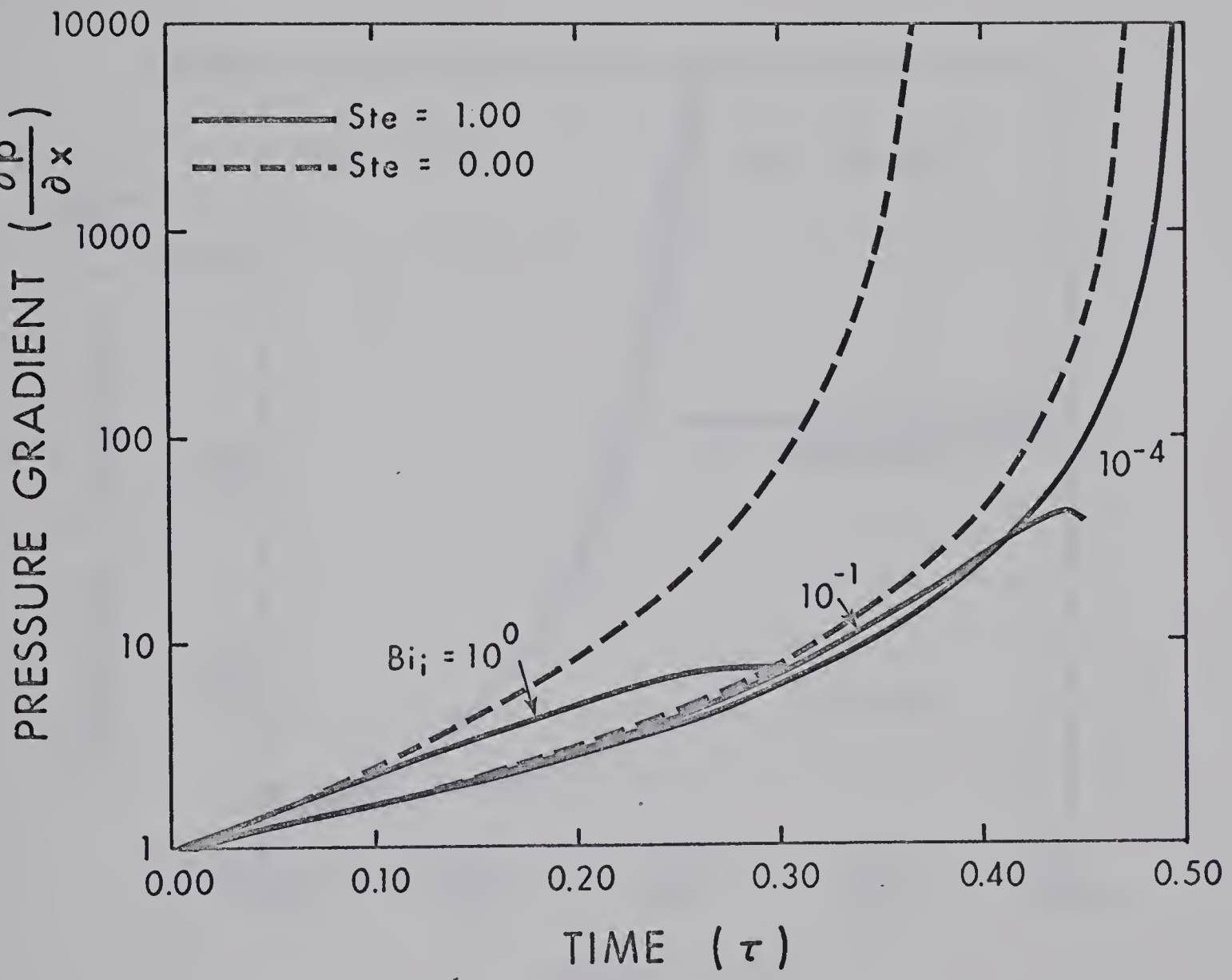

FIG. 3.2(c): EFFECT OF SENSIBLE HEAT AND CONVECTION ON PRESSURE GRADIENT

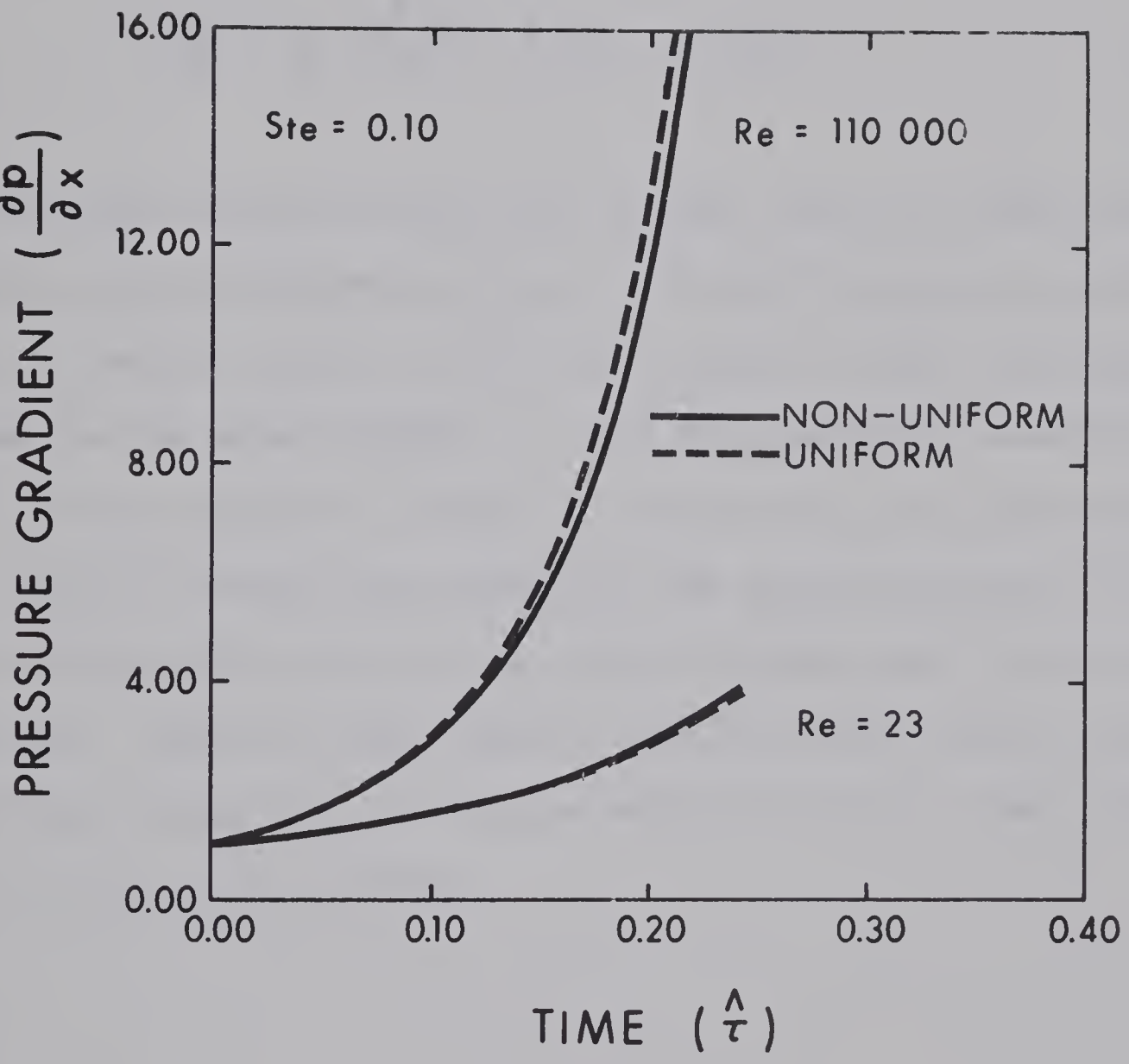

FIG. 3.3: PRESSURE STEEPENING IN A TRANSVERSE AIR FLOW

For a constant flow rate this may be equated to the ice-free value

$$\dot{Q}_{ni} = -\frac{R_1^4}{4\mu}\left(\frac{\partial P}{\partial X}\right)_{ni} \cdot \frac{\pi}{2} \quad .$$

Therefore

$$\frac{\partial p}{\partial x} = \frac{\pi}{2} \cdot \left(\frac{R_1}{R_*}\right)^4 \left[\int G(r_*, \theta)\, dS_*\right]^{-1} \quad .$$

Throughout the above analysis R_* is always taken at a value great enough to ensure convergence of $f_j(r_*, \theta)$ but small enough to permit motion of the arcs around the fictitious boundary to exert sufficient influence at the actual boundary. It was found worthwhile re-establishing R_* for each value of τ at which the pressure drop was calculated.

Figure 3.2 reveals the steepening of the pressure gradient for representative values of the Stefan and Biot numbers under uniform external convection. Figure 3.3 shows similar curves for each of the two transverse flows incorporating non-uniform convection under the same conditions as previously considered.

CHAPTER IV

DISCUSSION OF THEORETICAL RESULTS

The effect of sensible heat and external convection on ice growth under uniform conditions is shown in figures 2.4 (a), (b) and (c). The effect of sensible heat is revealed through comparison of the solid curves, corresponding to the inclusion of sensible heat effects, and the broken curves, corresponding to the neglect of sensible heat in the ice, that is, Stefan number equal to zero. It is important to note that $Ste_i = 0$ in this context does not imply that $(T_f - T_c) = 0$, rather that $L = \infty$ and/or $Cp_i = 0$. Mathematically it represents the complete neglect of sensible heat effects; that is the quasi-steady state situation treated by London and Seban [3].

The range of Biot numbers for which the results are plotted is effectively the full range of permissible Biot numbers. For very large Biot numbers the solution is asymptotic to the Dirichlet type of boundary condition ($Bi_i = \infty$). Thus the curve plotted for $Bi_i = 10^4$ is accurate for all very large Biot numbers ($Bi_i \geq 10^4$). In terms of real time, the solutions for very small Biot numbers are not asymptotic, but with reference to the normalized time scale where τ includes Bi_i, the curves are asymptotic to the solution for an adiabatic boundary condition ($Bi_i = 0$). Thus the curve plotted for $Bi_i = 10^{-4}$ is accurate for all smaller values of Bi_i as it tends to zero. This curve is given by the limit of equation 2.2-13 as Bi_i approaches zero, noting that under the same limit $a_o \to a$. Thus

$$\lim_{Bi_i \to 0} a = (1 - 2\tau)^{1/2}$$

which is seen to be independent of Ste_i. Physically this means that the ice forms so slowly that the temperature profile within the ice does not differ from the steady state profile, and sensible heat effects are negligible. The influence of sensible heat effects is most noticeable for large Biot numbers although it is evident from figures 2-4 that this influence is generally small. Since the results are generally accurate to α^2 an upper limit on the Stefan number of 0.3 (Fig. 2.4(b)) ensures that inaccuracies of 10% will not be exceeded even as the Biot number approaches infinity. For the ice-water system Stefan numbers greater than 0.3 represent coolant temperatures less than -54°F which, although possible, occur infrequently in engineering situations.

The minima revealed in figures 2.4 have no physical meaning but result from a singularity in the first order solution for a_1. Since all higher order solutions in a perturbation expansion are dependent on the zeroth order solution, it is to be expected that the higher order solutions exist only in the domain where the zeroth order solution exists. In this case the zeroth order solution, as given by equation 2.2-13, exists only for $1 \geq a_0 \geq 0$. Now as a first approximation

$$a = a_0 + \alpha a_1$$

where both α and a_1 are positive. Thus, if a is to approach zero it is apparent that a_0 must become negative. The solutions for a_0 and a_1 do not exist for a_0 less than zero, and in fact a_1 becomes infinite as a_0 approaches zero. This results in the minima of figures 2.4. Results

in the region of the minima are not considered valid.

If the tube is immersed in a transverse flow the convective boundary condition (Bi_i) varies circumferentially in a manner which depends on the external Reynolds number and on the Prandtl number of the cooling fluid. If conditions are such as to provide a close approximation to axi-symmetry, ice growth can be calculated using the results of Chapter II with the local Biot number for any azimuthal location. Thus, an interface shape which approximates the actual interface shape can be generated at any time. Since this method ignores the effects of azimuthal conductions in the ice, a good measure of the error is to compare the magnitudes of the radial and azimuthal conduction terms in the interface shape calculated (see Appendix A). Equation A-2 in Appendix A reveals that the error approaches zero for very larges values of the Biot number and for very small azimuthal variations as would be expected. Figure A.1 gives results for which the magnitude of the azimuthal conduction term is 10% of that of the radial conduction term.

Figures 2.5 and 2.6 show ice-water interface profiles for ice formation in a cooling air flow at two different Reynolds numbers. Figure 2.5 describes the lower Reynolds number situation which has a low mean Biot number. As is expected, moderate variations in the local Biot number result in significant variations in ice thickness. The radially-symmetric approximation seems reasonably valid in this case. Figure 2.6 presents similar results for a much higher Reynolds number and higher mean Biot number. Although the variations in ice thickness are less pronounced in this case, it can be readily seen from figure

2.6 that as lower interface radii are encountered the radially-symmetric assumption is doubtful. This is in complete agreement with the predictions of Appendix A.

One important engineering consideration in the formation of ice in a pipe is the effect of the reduced area for liquid flow in the pipe. Thus, for a fixed flow rate, the pressure gradient in the fluid will experience an increase as the flow area is reduced. Figures 3.2 (a, b, c) show the pressure gradient increase for the cases of uniform external convection of figures 2.4 (a, b, c). Under uniform convection, the pressure gradient is inversely proportional to the forth power of the interface radius. Figure 3.3 presents the results for the two cases of non-uniform convection as described in figures 2.5 and 2.6. It is apparent that for the time interval considered there is little difference between the pressure gradient calculated for non-uniform convection using the interface profiles of section 2.3, and that calculated assuming uniform convection at the mean Biot number of the transverse flow.

The analysis assumes that the water is not superheated. However the results may be considered valid for situations where

$$k_w \left(\frac{\partial T_w}{\partial R}\right)_A \ll k_i \left(\frac{\partial T_i}{\partial R}\right)_A \quad ,$$

or as an approximation

$$k_w \left(\frac{T_{wo} - T_f}{R_1}\right) \ll h \left(T_f - T_c\right) \quad .$$

Under conditions where the water is only heated by viscous dissipation the temperature in the water is given approximately by

$$(T_{wo} - T_f) = U_{av}^2/c_{pw}$$

from which it follows that viscous dissipation may be ignored if

$$\frac{k_w}{c_{pw}} \frac{U_{av}^2}{R_1} << h(T_f - T_c) ,$$

that is

$$U_{av}^2 << L(\frac{k_i}{k_w}) (\frac{c_{pw}}{c_{pi}}) Ste_i Bi_i .$$

Using the appropriate properties for ice and water it can be shown that for a pipe of radius A (in feet), the effect of viscous dissipation may be neglected if

$$Re \leq 10^7 A (Ste_i Bi_i)^{1/2} .$$

It is clear that dissipation will not normally be important unless Ste_i Bi_i, or α, is extremely small and/or the water velocity is very high. Physically a very small value of α implies either a very small temperature difference or a very small convective heat transfer coefficient. Either of these situations suggests very slow ice growth in which case even small energy contributions from viscous dissipation will have a significant effect. For a fixed flow rate very high water velocities will undoubtably occur as the ice-water interface approaches the tube axis. Thus results can be inaccurate when the water occupies only a small region, e.g. near the tube centerline. If the pressure drop is

constant, dissipation will be less important unless it cannot be initially ignored.

The analysis ignores circumferential conduction in the tube wall since it is reasonable to assume $w << R_1$ and isotherms are expected to be roughly circular. Therefore azimuthal temperature gradients will usually be small and will not generate significant heat fluxes in the azimuthal direction. In the radial direction

$$k_i \frac{\partial T}{\partial R}\Big|_{R_1} = k_m \frac{\partial T}{\partial R}\Big|_{R_1}$$

or approximately

$$k_i \frac{\Delta T_i}{R_1} \simeq k_m \frac{\Delta T_m}{w}$$

and hence

$$\frac{\Delta T_m}{\Delta T_i} \simeq \frac{k_i}{k_m} \frac{w}{R_1} .$$

Thus, assuming the tube is metallic it follows that $\Delta T_m << \Delta T_i$ and does not significantly alter the assumed boundary conditions. Since $c_{pm} < c_{pi}$ the effect of sensible heat in the metal is likewise insignificant.

Although the system of ice and water has been central throughout the analysis the discussion is not limited to such a system. The only restriction to be placed on any physical situation is that α must be less than unity, noting that the solution is in error by α^2.

PART II

EXPERIMENTAL INVESTIGATION

CHAPTER V

EXPERIMENTAL APPARATUS

The experimental apparatus employed was essentially that used by Freeborn [11] with certain modifications. It was considered as two systems; one for controlling the external boundary conditions and the other for the internal fluid flow (see fig. 5.1).

The external boundary condition was controlled by a closed system primarily composed of a reservoir, pump and piping which supplied the test section cooling jacket with a constant flow of the cooling agent (equal quantities of water and ethylene glycol). The coolant was stored in a 3.5 cu. ft. reservoir equipped with a cooling coil connected to a vapor compression refrigeration unit. The refrigeration capacity of one ton enabled the reservoir to be maintained at a constant temperature of -15°F. The reservoir supplied the cooling jacket through a one-inch diameter copper tubing recirculating system, containing a motorized three-way valve and pump.

A resistance bulb thermometer, (L 7033A Balco) located about one foot downstream of the three-way valve, was used with a resistance thermometer controller (Honeywell R 70870) to actuate the three-way valve (Honeywell Series 1616 three-way valve with M904 Modutol Motor). The pump recirculated the coolant from the jacket to the main reservoir and to the three-way valve which mixed some returning coolant with -15°F coolant direct from the reservoir to maintain the temperature set on the resistance thermometer controller. The reservoir and piping were insulated to prevent heat leakage to the system.

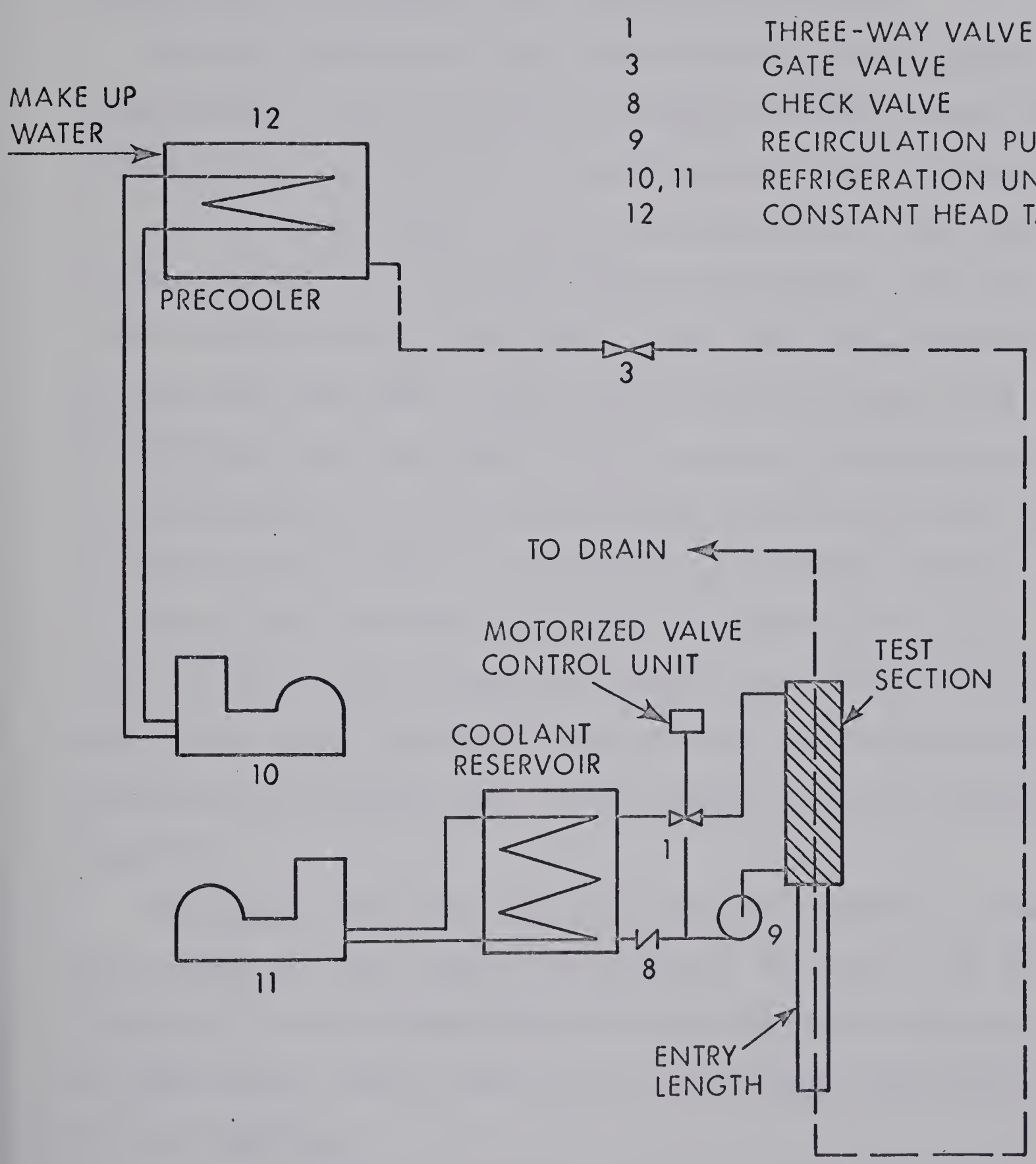

FIG. 5.1: SCHEMATIC OF EXPERIMENTAL APPARATUS

The water flow was governed by an open system consisting of two constant-head storage tanks, supply and discharge piping, motorized three-way valve, flow meter, entry length and test section.

Water was stored in the larger header tank (9 cubic feet) where it was cooled by a coil around which an icebank of fixed thickness was allowed to form. Thus the water was maintained at a constant temperature near the freezing point. The coil was connected to a vapor-compression refrigeration unit with a one-half ton capacity. The water in the second and smaller header tank (1 cubic foot) was maintained at the water main temperature. Water from both tanks was piped to the motorized three-way valve where the "cold" water was trimmed to the desired temperature by mixing with the "warm" water from the small tank. The water was fed through one inch diameter copper tubing, through a flow meter (Fisher and Porter Ratosight) and controlling gate valve into a six foot section of three inch diameter copper tubing; the last three feet of which constituted the test section. This section was surrounded by the cooling jacket and the complete system was thermally insulated.

The complete test section and inlet piping were mounted on a frame which enabled the test section to be rotated to, and held at, any inclination. To allow freedom of operation the inlet water connection was made through a swivel joint and the coolant system incorporated flexible couplings.

CHAPTER VI

INSTRUMENTATION

The prime instrumentation problem involved measuring the ice thickness inside a long vertical pipe completely surrounded by an insulated cooling jacket. In the general case the ice thickness has both axial and azimuthal variation.

Gort [9] measured the ice thickness with a stainless steel probe from which mechanical arms were deployed to contact the ice water interface. The device was only suitable for radially symmetric situations although it did permit an axial traverse.

Freeborn [11] was successful at measuring ice thickness with an ultrasonic technique. However, attempts at obtaining axial profiles met with little success except in regions where axial variations in the ice thickness were very small. The ultrasonic technique has the very definite advantage of measuring ice thickness directly as opposed to measuring the distance from the probe to the ice-water interface. The latter requires knowledge of the exact location of the probe relative to the pipe centerline.

In order to study both axial and azimuthal variations in the ice thickness a new finger-type mechanical probe was designed (fig. 6.1). The device was intended to operate as a continuous reading profilometer to be drawn axially through the pipe. Variations in the ice thickness cause radial movement of the sensing arm which results in a corresponding axial movement of the transducer core. This causes a change in the electrical signal from the voltage transducer (Ametek 400-3K-9EL) proportional to the radial displacement. Calibration of the device with a

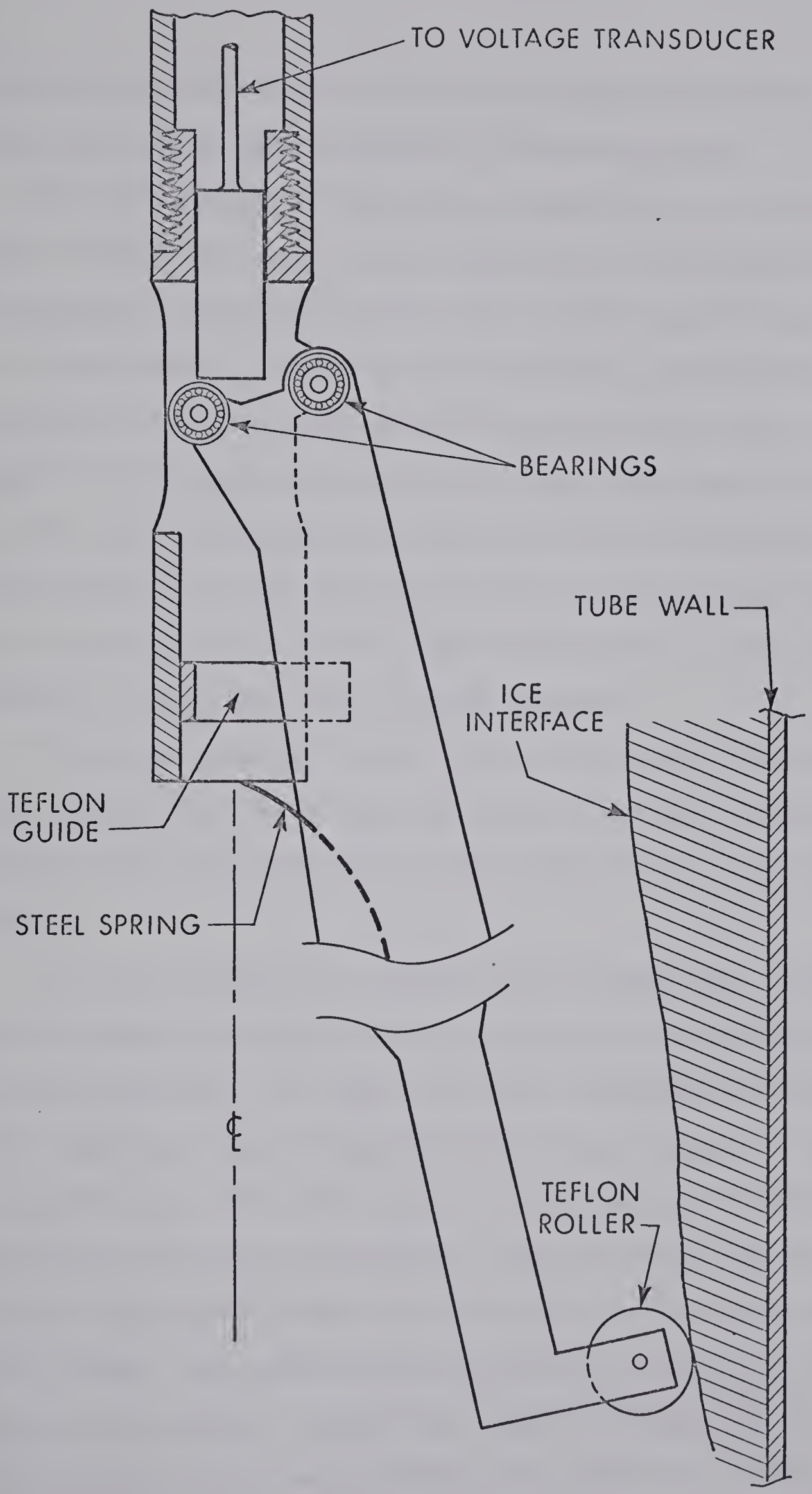

FIG. 6.1: SCHEMATIC OF FINGER PROFILOMETER

micrometer screw revealed an effective resolution better than 0.005 inches and readings were repeatable to within this limit.

The axial position of the probe was controlled by a reversing D.C. motor driving a lead screw to which the one-half inch diameter probe was attached. The position of the probe was then monitored by a forty-turn potentiometer: a change in potential from a prescribed datum indicated the distance of the probe from the test section entry. The signals from the potentiometer and the voltage displacement transducer were then used to drive an X-Y recorder with the ice thickness plotted on the vertical axis and the axial position on the horizontal axis. By this means an axial profile of the ice thickness, for any azimuthal location at a particular time, could be generated.

To generate azimuthal profiles the probe was set at the desired axial locations and with a time base on the X-Y plotter the probe was rotated through 180 degrees with a five second pause at each azimuthal location.

In order to maintain the desired coolant temperature, a resistance bulb thermometer was located in the coolant recirculating line, as previously mentioned. The signal from this thermometer was transmitted to the temperature control mechanism where it was compared to a pre-set control value. The error signal, if any, energized the motor controlling the three-way valve movement, thus positioning the valve for a higher proportion of either the -15°F coolant or the warmer recirculating coolant. The three-way valve operation for control of the water temperature was similar, except that a copper-constantan thermocouple sensor was used and the valve movement was controlled manually by use

of a three-way toggle switch.

Further instrumentation consisted of copper constantan thermocouples situated in the water inlet region, six and nine inches before the test section entry, and in the coolant recirculation piping immediately downstream from the cooling jacket. In an attempt to measure the temperature gradient across the pipe wall in the test section, thermocouples were located on the inner and outer surfaces of the test section in three locations. Readings were obtained using either a millivolt potentiometer (Leeds & Northrup 8686) or a digital voltmeter (Hewlett-Packard 3440A).

CHAPTER VII

EXPERIMENTS

7.1 No-Flow Test

Initially a test was conducted at zero flow rate and zero superheat ($\sigma = 0$) in order to make a comparison with theory and other experiments (see Freeborn [11]).

Before the test, the water in the large header tank was cooled over a prolonged period. The test section was completely drained and set in the vertical position. A traverse was made with the profilometer, giving a datum line on the X-Y recorder for the no-ice condition. The cooling system recirculating pump was then started with the coolant temperature control set at approximately -5°F. After waiting to ensure the stabilization of the coolant temperature the valve to the test section was opened until water began to emerge from the discharge line. The valve was then closed and the timer started. Axial traverses were made at approximately three minute intervals and thermocouple readings were recorded as the traverse was being made. At the conclusion of the test the coolant temperature control was set above the freezing point and warm water passed through the test section, melting the ice. After the ice was melted the water was shut off and the test section drained.

7.2 Inclined Laminar Flow Tests

Next a series of tests was conducted to determine the influence of flow, superheat and angle of inclination on the rate of ice formation.

With the coolant temperature control set above the freezing point, the flow was directed through the test section and adjusted to get the desired flow rate and superheat ratio with the test section set at the desired inclination. The flow was then discharged before reaching the test section and the test section was prepared as described in the no-flow test. With the system in a steady condition the flow was switched back through the test section and the timer started. Axial profiles and temperatures were recorded as before. In addition, some azimuthal traverses were made with the probe at a fixed axial location. Periodically, the flow rate was checked by measuring the amount of water discharged over a timed interval. At the end of the test the ice was melted and the section drained as previously described.

CHAPTER VIII

DISCUSSION OF EXPERIMENTAL RESULTS

8.1 No-Flow Test

This experiment was to be conducted without flow and with zero superheat as previously mentioned. Ideally, the situation is that of a liquid flowing at its freezing temperature in a pipe cooled by uniform external convection (i.e. fully developed ice formation).

In actual fact the water temperature was approximately 35°F with a superheat ratio of 0.09. Figure 8.1 shows the results of the axial traverses for this test. There are several reasons for the axial variations in the ice thickness. Near the entry region the effects of axial conduction in the ice would tend to reduce the rate of ice formation as can be seen from the graph near z = 0. Secondly, since the water is not initially at the freezing temperature there must be some effect due to natural convection and this effect will have an axial dependency contributing to axial variations in the ice thickness at any time. A third contributing factor is the probability that the external heat transfer coefficient is non-uniform in the axial direction.

It should be noted that in figure 8.1 the graph scaling is such that ice thickness variations are greatly exaggerated. Figure B.1 of Appendix B shows the same curve in the proper perspective. Here it becomes apparent that the experiment is in fact very close to fully developed ice formation.

Figure 8.2 shows the test results at the axial location where Freeborn [11] obtained results with the ultrasonic profilometer. Also

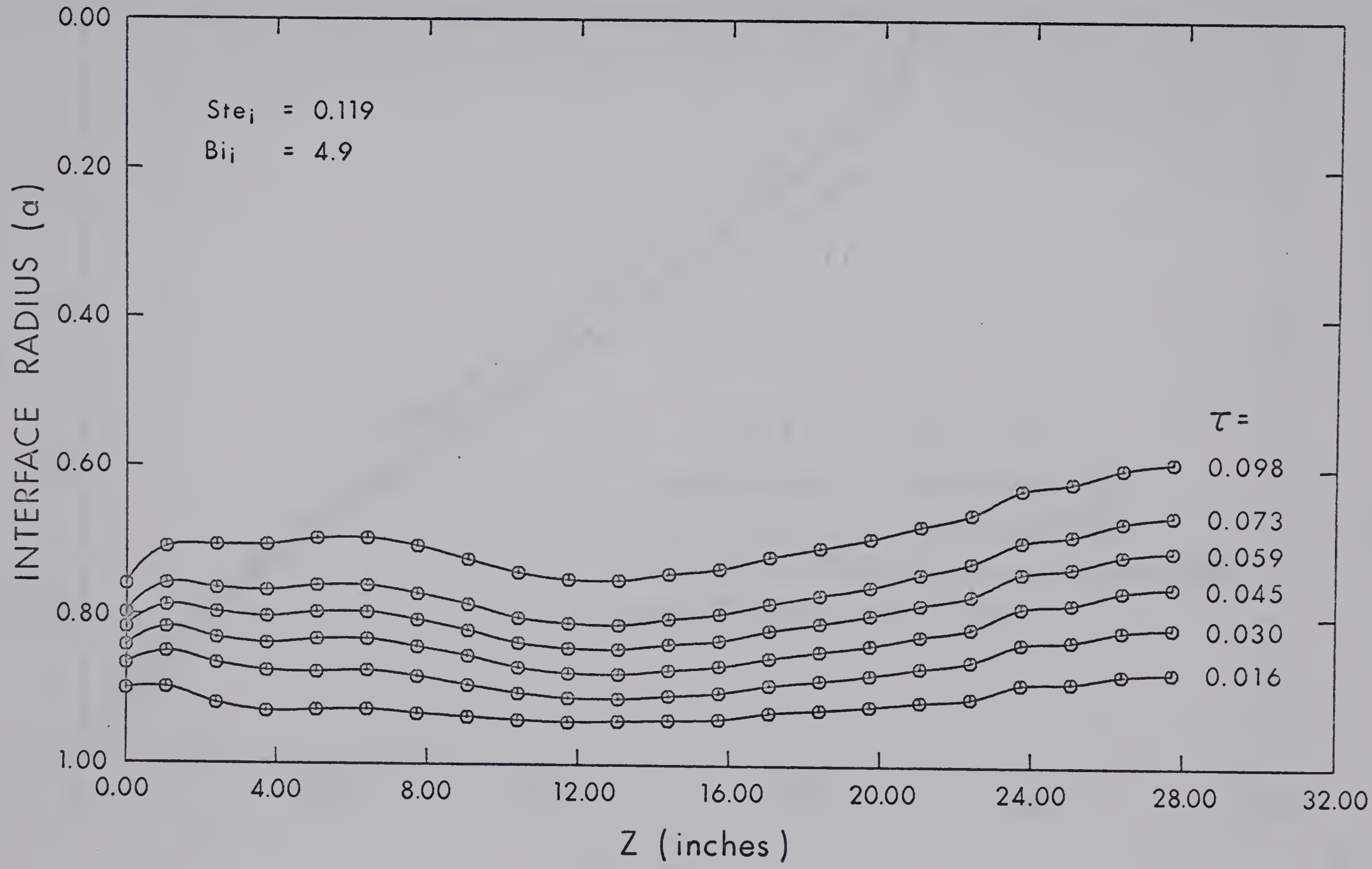

FIG. 8.1: AXIAL PROFILES

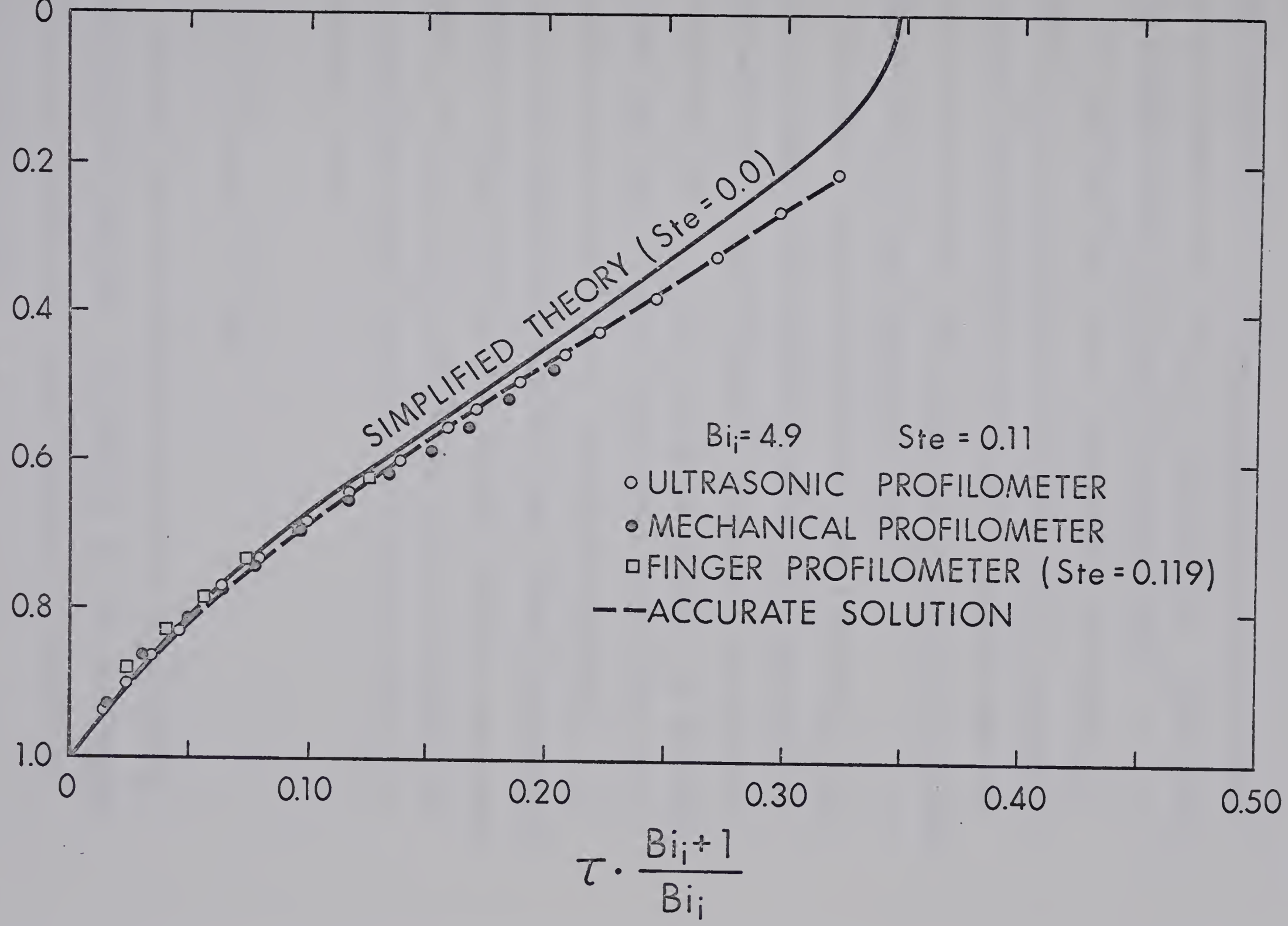

FIG. 8.2: COMPARISON WITH PREVIOUS RESULTS

shown are the results of Freeborn's no-flow, zero superheat test and the corresponding results from Gort's [9] experiments. There is very good agreement between the results of all three methods.

The solid and broken curves in figure 8.2 are the zeroth order and first order correct theoretical solutions for fully developed ice formation as developed earlier in this thesis. The first order solution is terminated short of the extremum and is seen to be in excellent agreement with all of the experimental results.

An attempt was made to determine the external heat transfer coefficient by measuring the temperature gradient across the pipe wall. There were inner and outer thermocouples installed at three locations but complete failures occurred at two of the locations. At the third location there were two adjacent thermocouples on the inside wall of the pipe but their readings were in considerable disagreement. Consequently this method of establishing the heat transfer coefficient was abandoned. Because of the excellent agreement between the experimental results of this test and the corresponding results of Freeborn [11], the external heat transfer coefficient was assumed to be the same as in Freeborn's work.

8.2 Inclined Laminar Flow Tests

Tests were run at four different test section inclinations for laminar flows with superheat. The results of the tests are presented in figures 8.3 through 8.13. In each case the axial variables are nondimensionalized to give

$$z = Z/Pr\ Re\ R_1 \quad .$$

The inclination of the test section is γ given in degrees from the horizontal. In each inclined test the axial profiles were taken on the lower wall of the pipe.

Initially, it had been planned to keep the Reynolds number and superheat ratio constant throughout the tests and explore, through the angle of inclination, the effects of natural convection. Great difficulty was experienced in controlling the superheat ratio due to the time lag between operation of the three-way mixing valve and corresponding response in the inlet water temperature. Similarly, some difficulty was experienced in maintaining the desired Reynolds number in each test. The resulting scatter in these two parameters makes a strict analysis of the results, with respect to the effect of inclination, very difficult. However the results allow some general conclusions to be drawn about the nature of ice formation under these conditions.

Figures 8.3, 8.5, 8.8 and 8.11 are the axial profiles at various times for each test. In each case they reveal the existence of an asymptotic steady state condition near the entry region. Further downstream where the heat had been largely removed from the water, the profiles indicate that the situation was still a transient one. The ice thickness is expected to increase monotonically with increasing z for the vertical case ($\gamma = 90°$), and although the inclined cases are more difficult to analyze, a similar variation may be expected in these cases too. However the axial profiles for small times reveal that the ice thickness is not monotone. The strong similarity between the first

profiles in all four tests suggests axial variations in the heat transfer coefficient and/or the mean coolant temperature. This is supported by the fact that the exit region for the coolant in the cooling jacket was located near the water entry region on the same side of the test section as the profiles were obtained. This suggests that improved circulation in the cooling jacket near the exit results in a higher Biot number which accounts for a thickening in the ice profile in that region. At later times the effect of axial variations in the Biot number is reduced due to axial conduction in the ice layer, and the profiles reveal the expected monotonicity.

Figures 8.4, 8.6, 8.9 and 8.12 are simply cross-plots from the corresponding axial profiles at various axial locations. Once again the asymptotic steady state situation is revealed for small values of z and the purely transient nature is exhibited for larger values of z. The ice thickness at any axial location is expected to be monotonically increasing with time. In each of the tests it is observed that this is not the case for the smallest value of z plotted. This is due to the fact that when water first enters the test section the entire section has been cooled to the temperature of the coolant. Initially therefore the boundary condition is a Dirichlet type and the ice forms more rapidly than it would under the convective boundary condition. For small z this initial growth exceeds the eventual steady-state thickness and, as this quantity of ice cannot be supported by the convective boundary condition, the excess melts away at later times. At larger values of z, although the initial ice growth is accelerated, the effect is not so

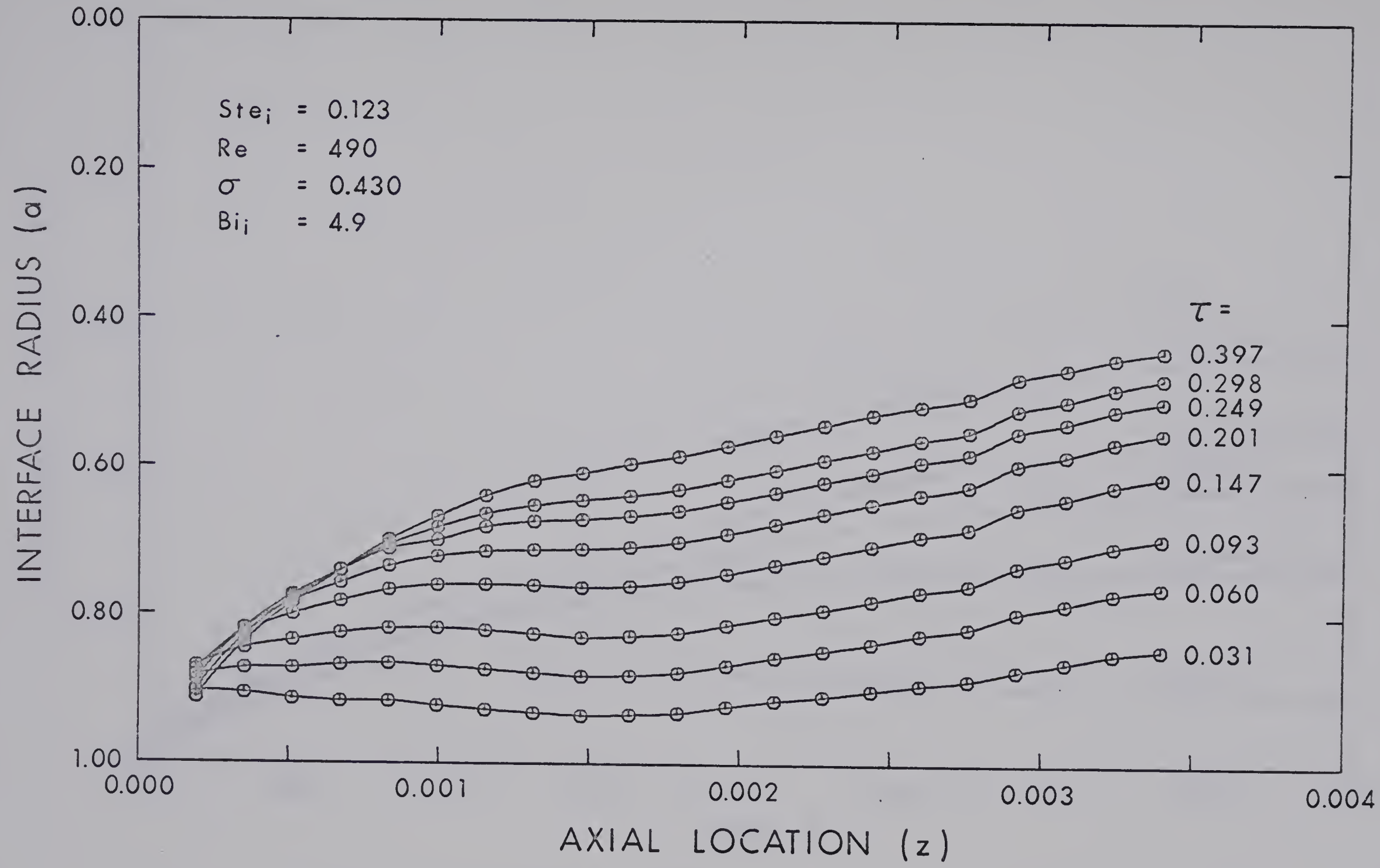

FIG. 8.3: AXIAL PROFILES $\gamma = 90^0$

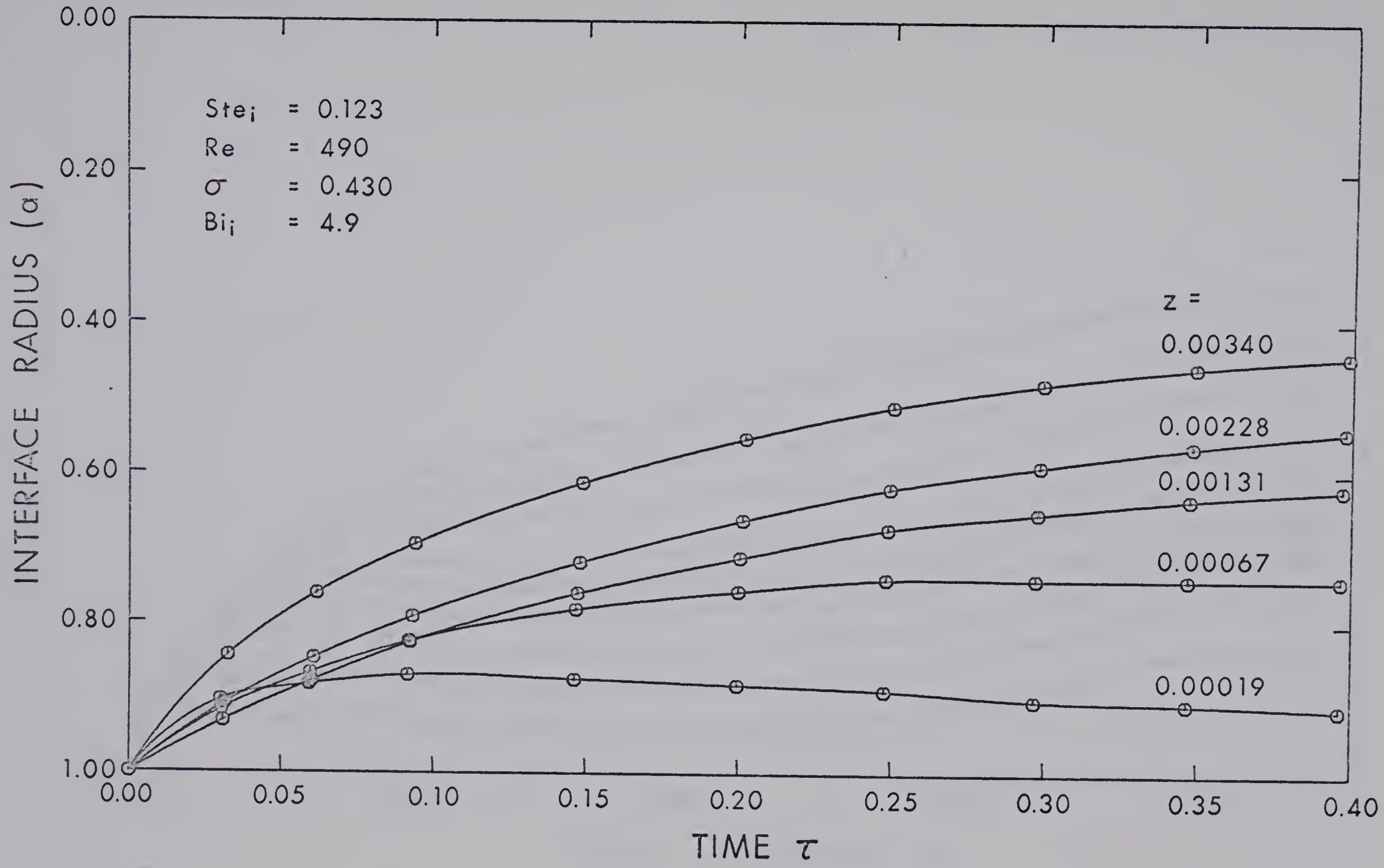

FIG. 8.4: INTERFACE HISTORY $\gamma = 90^0$

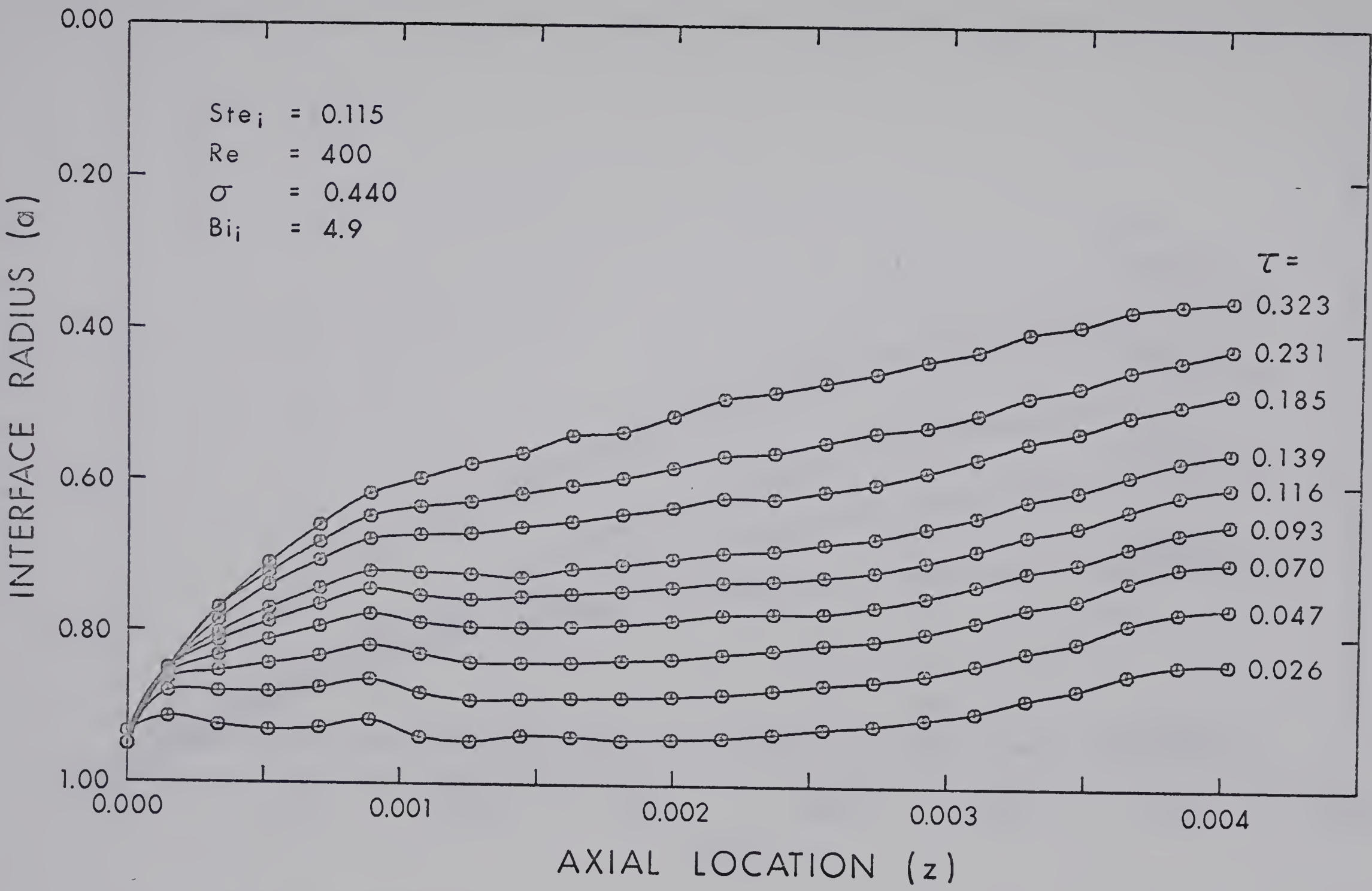

FIG. 8.5: AXIAL PROFILES $\gamma = 30^0$

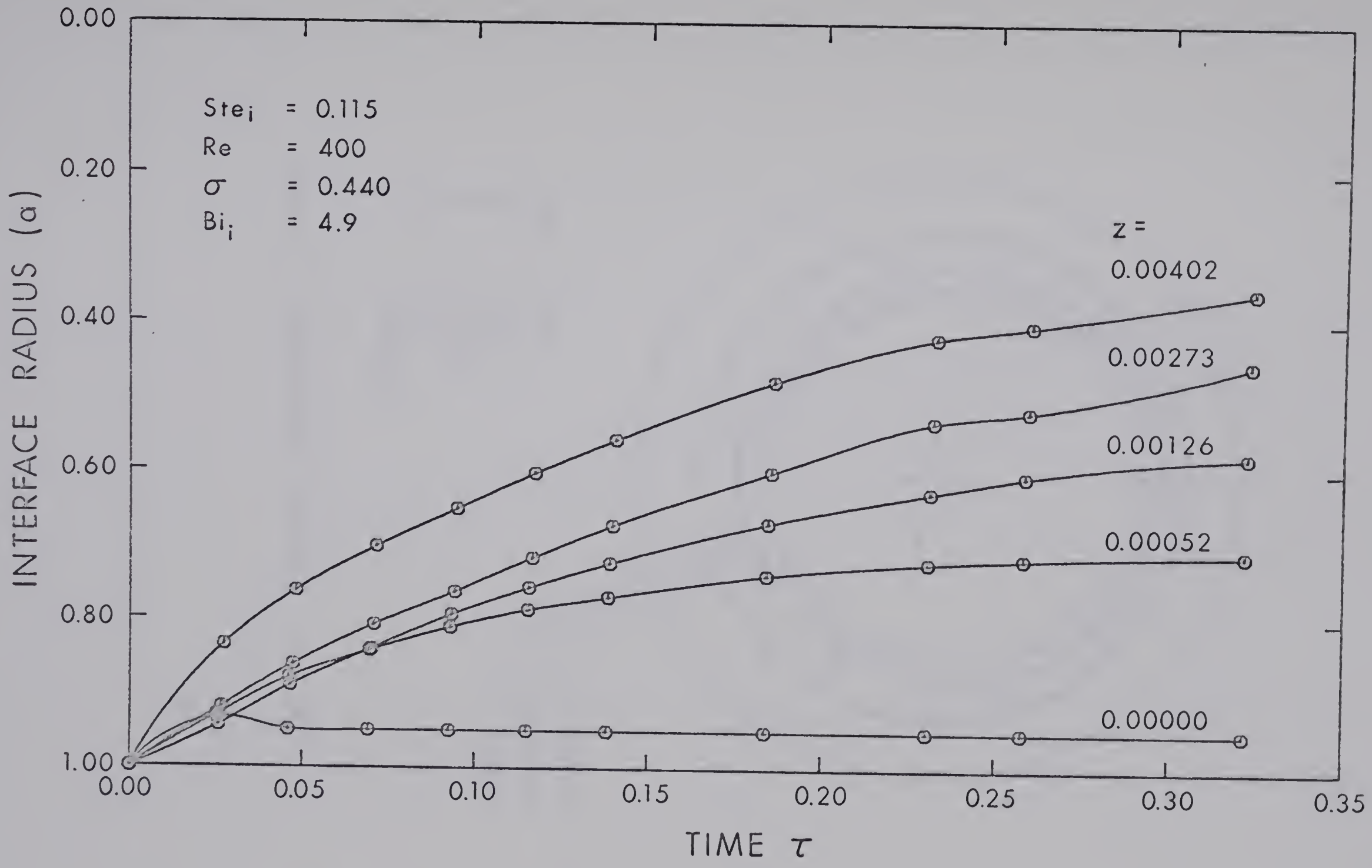

FIG. 8.6: INTERFACE HISTORY $\gamma = 30^0$

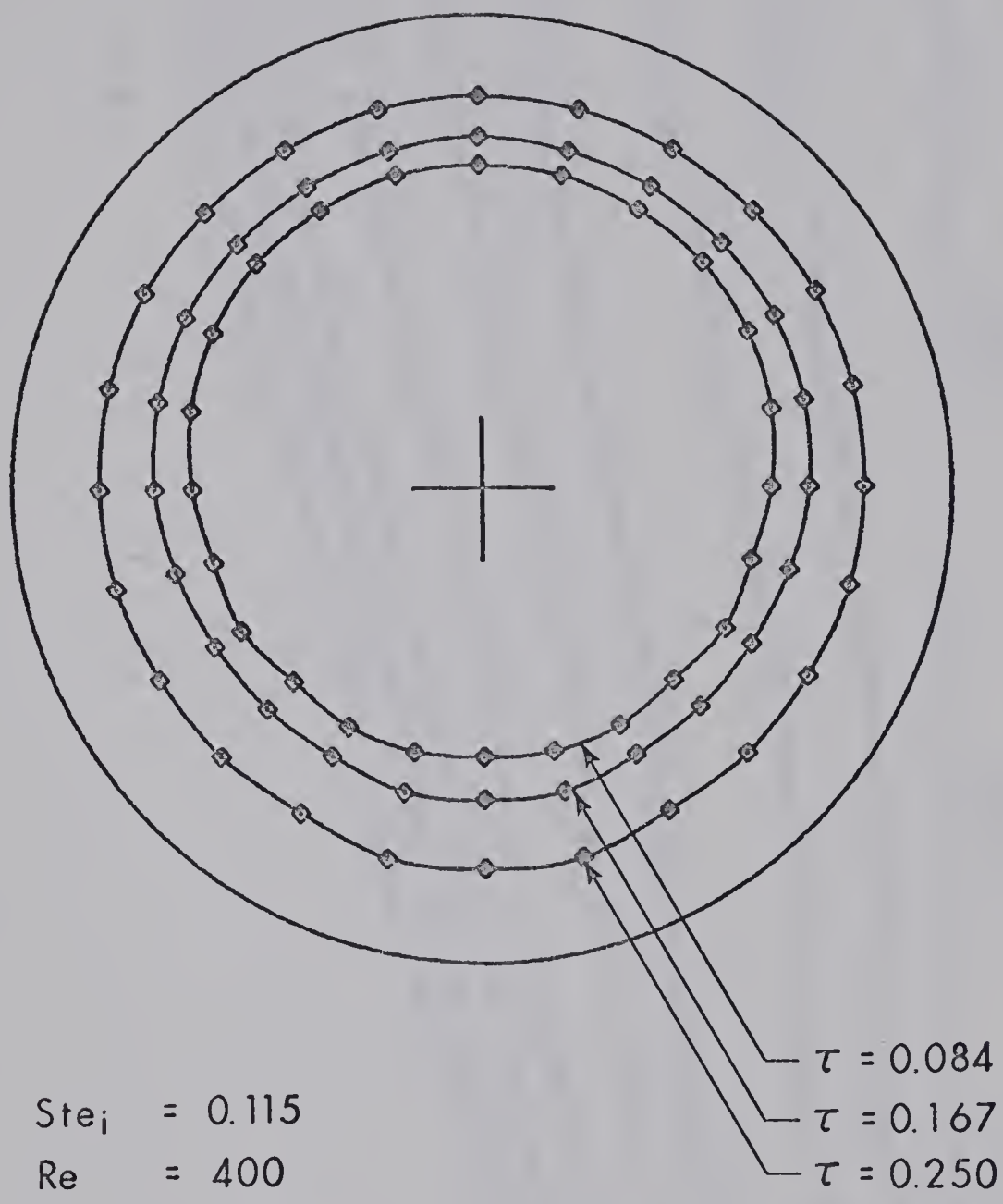

Ste_i = 0.115
Re = 400
σ = 0.440
Bi_i = 4.9
z = 0.00236

FIG. 8.7: AZIMUTHAL PROFILES $\gamma = 30^0$

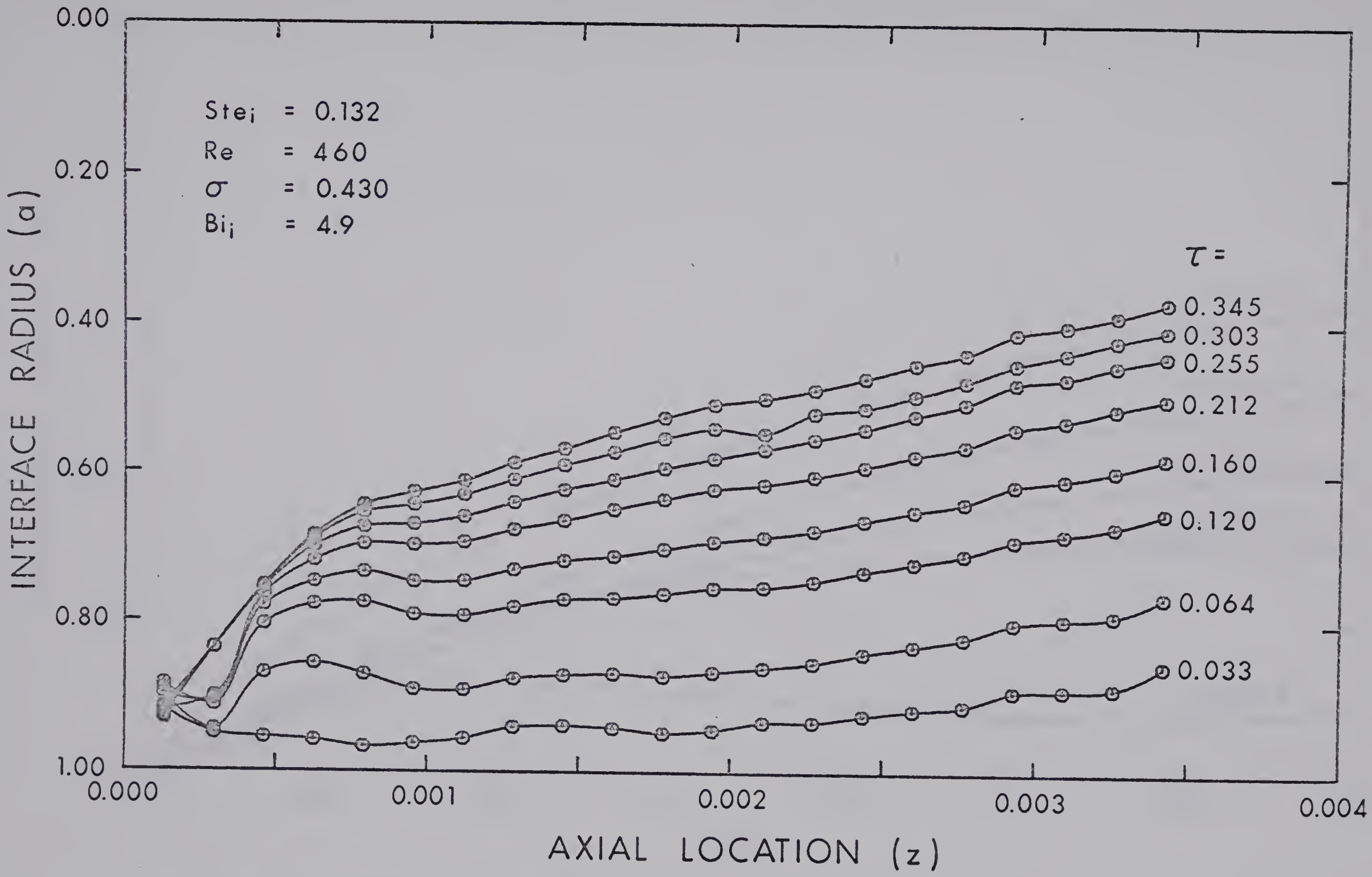

FIG. 8.8: AXIAL PROFILES $\gamma = 10^0$

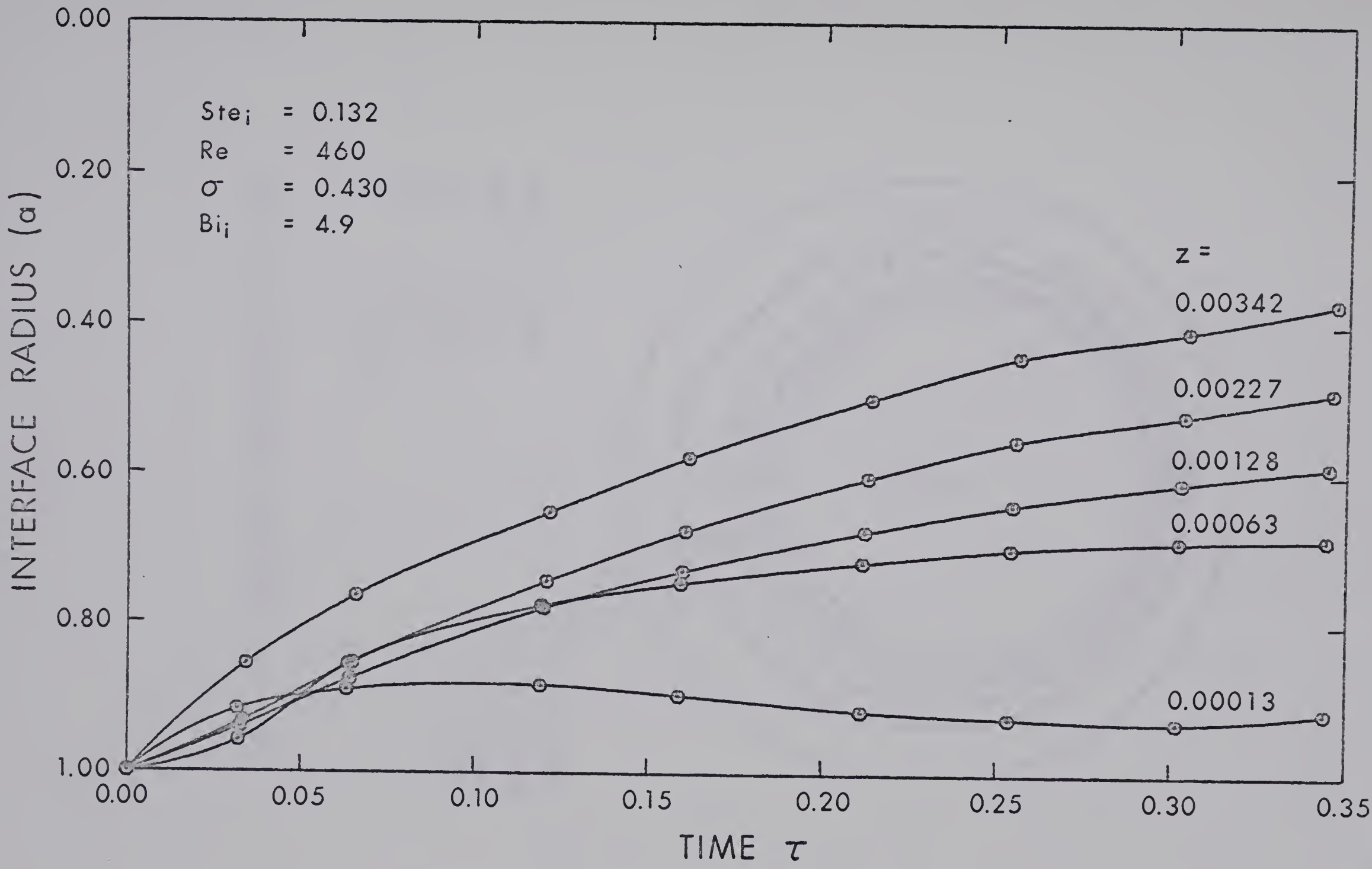

FIG. 8.9: INTERFACE HISTORY $\gamma = 10^0$

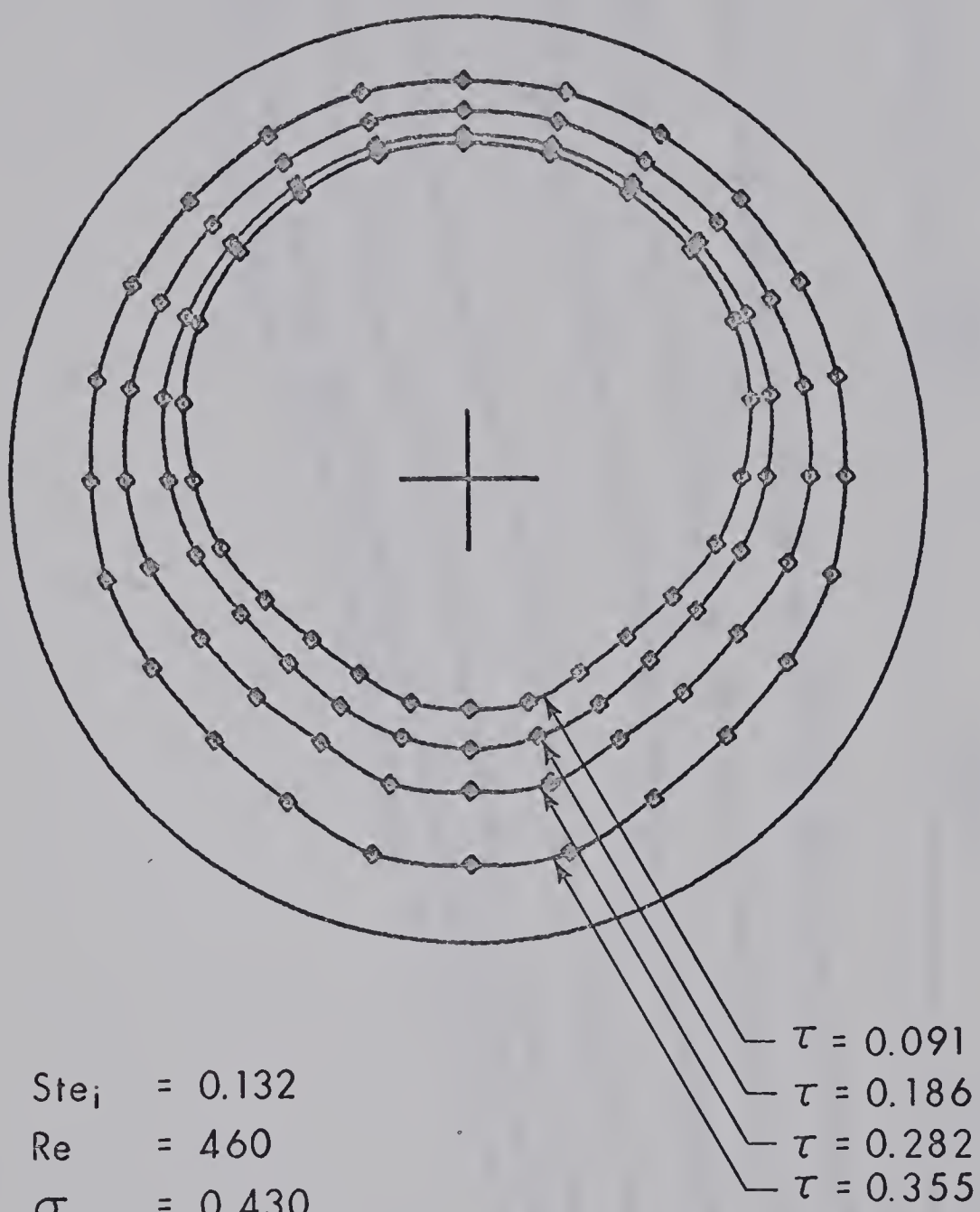

Ste_i = 0.132
Re = 460
σ = 0.430
Bi_i = 4.9
z = 0.00211

FIG. 8.10: AZIMUTHAL PROFILES $\gamma = 10^0$

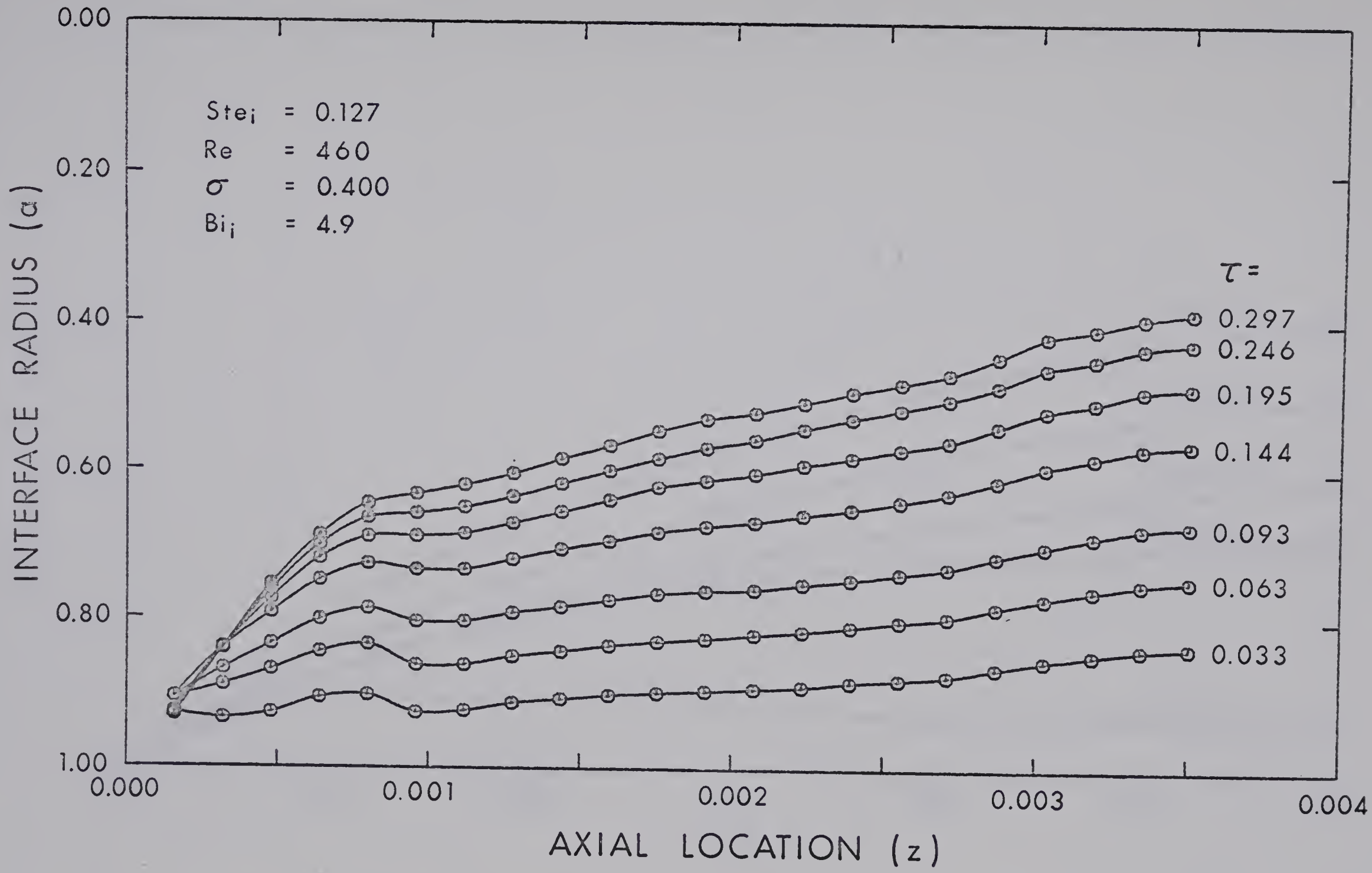

FIG. 8.11: AXIAL PROFILES $\gamma = 0^0$

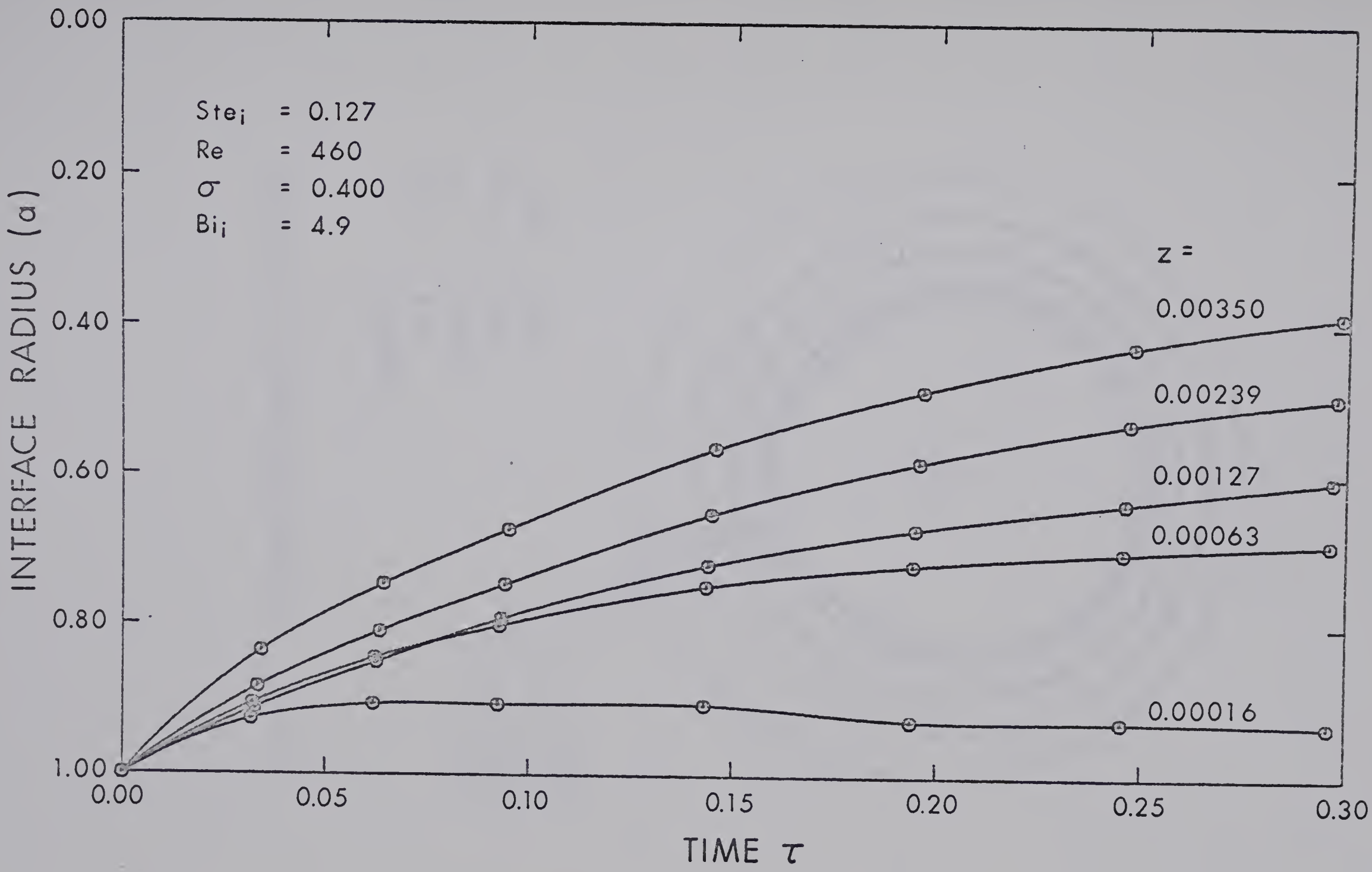

FIG. 8.12: INTERFACE HISTORY $\gamma = 0^0$

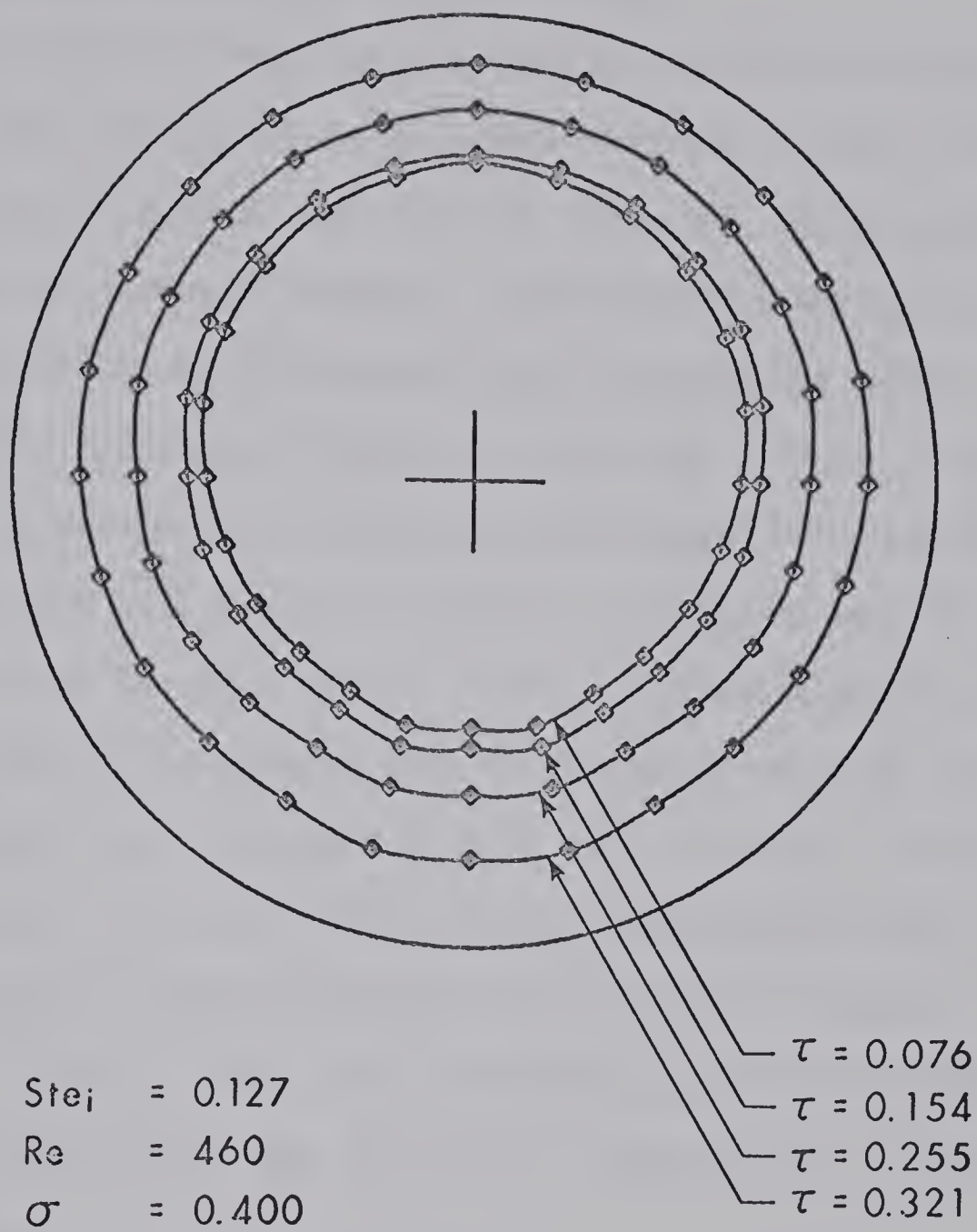

Ste_i = 0.127
Re = 460
σ = 0.400
Bi_i = 4.9
z = 0.00192

FIG. 8.13: AZIMUTHAL PROFILES $\gamma = 0^0$

obvious due to the fully transient behavior at these locations and the absence of significant superheat to cause melting.

Assuming a radially symmetric heat transfer coefficient around the test section, any asymmetry in the azimuthal profiles for the inclined tests would be due to natural convection in the water. At any particular inclination the degree of asymmetry indicates the importance of free convection for the given superheat ratio and Reynolds number. From the azimuthal profiles of figures 8.7, 8.10 and 8.13 it is apparent that free convection has a considerable effect under the experimental conditions. In each case the ice is thicker on the lower wall of the test section than on the top or sides. With a constant Reynolds number and superheat ratio it is expected that the asymmetry would be greatest for the horizontal case. Figures 8.7, 8.10 and 8.13 reveal that while the asymmetry for $\gamma = 0°$ and $\gamma = 10°$ is considerably greater than that for $\gamma = 30°$, there is little difference in the degree of asymmetry displayed for $\gamma = 0°$ and $\gamma = 10°$. This is probably due to the fact that the superheat ratio for the test at $\gamma = 0°$ is significantly less than that for $\gamma = 10°$.

PART III

CONCLUSIONS

CHAPTER IX

CONCLUDING REMARKS

9.1 Conclusions

This thesis has presented a theoretical analysis of ice formation in a convectively-cooled circular tube in the absence of superheat in the water. It has also presented experimental results for ice formation within a convectively-cooled inclined tube in the presence of body forces.

The theoretical analysis accommodates the effect of sensible heat in the ice through a perturbation expansion in a typically small parameter. Generally, sensible heat effects were found to be small and were shown to be of greatest importance in situations when the cooling is very rapid, i.e. $Bi_i \gg 1$ and/or $(T_f - T_c) \gg 1$.

The analysis was applied to a particular asymmetric convective cooling situation (a pipe in a cross-flow) which could be treated as quasi-radially symmetric. A semi-analytic technique was developed to analyze the flow of water within the asymmetric ice shells which develop in such situations.

Experiments were carried out for ice formation within a pipe under both symmetric (vertical) and asymmetric (inclined) test conditions. A specially-designed finger profilometer enabled both axial and azimuthal profiles of the ice-water interface to be obtained. Profiles were first obtained for the symmetric case of ice formation with no flow and no superheat in the water. The results were found to be in excellent agreement with previous results which had been obtained by

two different techniques. From this agreement it can be concluded that the experiments are reproducible.

Results were then obtained for the case of superheated water flowing in an inclined tube. Ice growth under these conditions is not symmetric and therefore both axial and azimuthal traverses were performed. Although theoretical predictions for ice growth under these conditions are not available for comparison, the results appeared consistent with expectations. For the region near the entry to the test section an asymptotic steady-state interface was revealed in all tests in which superheat was present. Further downstream the situation was found to be fully transient and approaching fully-developed ice formation. The azimuthal profiles of the ice-water interface revealed that natural convection in the water is of considerable importance under the test conditions employed. It was observed that the asymmetry in the profiles was greatest for inclinations very near the horizontal. In all inclined tests the ice formed most rapidly on the lower wall of the test section.

9.2 Suggestions for Further Work

The finger profilometer proved very successful for obtaining both axial and azimuthal interface profiles. It is felt that this method could be used to obtain results for a very extensive experimental study of ice formation in pipes. The existing apparatus would need improvements to allow better control over inlet and boundary conditions. For a very large test program it would also be desirable to automate the data recording through the use of magnetic tape recording devices compatible with the University computing facilities.

REFERENCES

REFERENCES

1. BRUSH, W.W., "Freezing of Water in Subaqueous Mains Laid in Salt Water and in Mains and Services Laid on Land", Journal of the American Water Works Association, Vol. 3, 1916, pp. 962-980.

2. PEKERIS, C.L. and SLICHTER, L.B., "Problems of Ice Formation", J. App. Phys., Vol. 10, 1939, pp. 135-137.

3. LONDON, A.L. and SEBAN, R.A., "Rate of Ice Formation", Trans. A.S.M.E., Vol. 65, 1943, pp. 771-778.

4. KREITH, F., and ROMIE, F., "A Study of the Thermal Diffusion Equation with Boundary Conditions Corresponding to Solidification or Melting of Materials Initially at the Fusion Temperature", Phys. Soc. Proc., Sect. B, Vol. 68, Pt. 5, May 1955, pp. 277-291.

5. ALLEN, D.N. DE G and SEVERN, R.T., "The Application of Relaxation Methods to the Solution of Non-Elliptic Partial Differential Equations. III. Heat Conduction, with Change of State, in Two Space Dimensions", Quart. J. Mech. App. Math, Vol. 15, 1962, pp. 53-62.

6. POOTS, G., "On the Application of Integral-Methods to the Solution of Problems Involving the Solidification of Liquids Initially at Fusion Temperature", Int. J. Heat Mass Transf., Vol. 5, 1962, pp. 525-531.

7. ZERKLE, R.D. and SUNDERLAND, J.E., "The Effect of Liquid Solidification in a Tube Upon Laminar-Flow Heat Transfer and Pressure Drop", J. H. Transfer, Vol. 90, 1968, pp. 183-190.

8. DesRUISSEAUX, N., and ZERKLE, R.D., "Freezing of Hydraulic Systems", Paper presented at the A.I.Ch.E.-A.S.M.E. Heat Transfer Conference and Exhibit, Philadelphia, Pa., August 11-14, 1968.

9. GORT, C., "Preliminary Study of Ice Formation in a Vertical Pipe", M.Sc. Thesis, University of Alberta, Edmonton, Alberta, June 1968.

10. ÖZISIK, M.N., and MULLIGAN, J.C., "Transient Freezing of Liquids in Forced Flow Inside Circular Tubes", presented at A.S.M.E. Winter Annual Meeting, December 1-5, 1968, Paper No. 68-WA/HT-7.

11. FREEBORN, R.D.J., "Ice Formation in Vertical Tubes with Convective Boundary Conditions", M.Sc. Thesis, University of Alberta, Edmonton, Alberta, Spring 1969.

12. KNUDSEN, J.G. and KATZ, D.L., "Fluid Dynamics and Heat Transfer", McGraw-Hill, New York, 1958, pp. 497-501.

13. CHENG, K.C., "Laminar Flow and Heat Transfer Characteristics in Regular Polygonal Ducts", Proc. 3rd Int. H.T. Conf., A.I.Ch.E., Chicago, 1966, pp. 64-76.

14. SPARROW, E.M. and HAJI-SHEIKH, A., "Flow and Heat Transfer in Ducts of Arbitrary Shape with Arbitrary Thermal Boundary Conditions", J. Heat Transf., Vol. 88, No. 4, 1966, pp. 351-358.

15. TAO, L.N., "Method of Conformal Mapping in Forced Convection Problems", International Developments in Heat Transfer, A.S.M.E., 1961, pp. 598-606.

16. BOLEY, B.A., "The Analysis of Problems of Heat Conduction and Melting", High Temperature Structures and Materials: Proceedings of the Third Symposium on Naval Structural Mechanics, Pergamon Press, London, 1963, pp. 260-315.

APPENDIX A

THE QUASI-RADIALLY SYMMETRIC APPROXIMATION

APPENDIX A

THE QUASI-RADIALLY SYMMETRIC APPROXIMATION

The heat flux vector for two dimensional conduction is given by

$$\bar{q} = -k \nabla\phi = q_r \bar{e}_r + q_\theta \bar{e}_\theta$$

Therefore the ratio of q_θ to q_r will be a measure of the error in the quasi-radially symmetric analysis. Using the zeroth order approximation we find from equation 2.2-7

$$\phi = \frac{-Bi_i}{1 - Bi_i \ln a} \ln \frac{r}{a} \quad .$$

Thus if Bi_i is a function of θ

$$q_\theta = \frac{1}{r}\frac{\partial\phi}{\partial\theta} = \frac{1}{r}\frac{dBi}{d\theta}\frac{\partial\phi}{\partial Bi} + \frac{1}{r}\frac{da}{d\theta}\frac{\partial\phi}{\partial a}$$

Evaluating at r = a this gives

$$q_\theta|_a = \frac{da}{d\theta}\frac{1}{a^2}\frac{Bi}{1 - Bi \ln a} \quad .$$

At the same location

$$q_r|_a = \frac{\partial\phi}{\partial r}|_a = \frac{-1}{a}\left(\frac{Bi}{1 - Bi \ln a}\right)$$

The ratio of q_θ to q_r at a is therefore given by

$$E = \frac{\frac{1}{a}\frac{\partial\phi}{\partial\theta}\Big|_a}{\frac{\partial\phi}{\partial r}\Big|_a} = -\frac{1}{a}\frac{da}{d\theta} \quad . \qquad \text{A-1}$$

The interface location a is found from equation 2.2-13 which can be rearranged to give

$$\frac{Bi + 2}{Bi} = \left[\tau\left(\frac{1 + \hat{Bi}_i}{\hat{Bi}_i}\right) - \frac{a^2 \ln a}{2}\right]\left[\frac{4}{1 - a^2}\right]$$

or $f(Bi) = g(a)$.

Differentiating with respect to θ we find

$$\frac{dBi}{d\theta}\left(\frac{\partial f}{\partial Bi}\right) = \frac{da}{d\theta}\left(\frac{\partial g}{\partial a}\right)$$

from which

$$\frac{da}{d\theta} = -\frac{a^2 - 1}{2a\, Bi_i}\left(\frac{1}{1 - Bi_i \ln a}\right)\frac{dBi_i}{d\theta} \quad .$$

Substituting into A-1 for $\frac{da}{d\theta}$ yields the result

$$E = \frac{1 - a^2}{2a^2}\left(\frac{1}{Bi_i - Bi_i^2 \ln a}\right)\frac{dBi}{d\theta} \quad . \qquad \text{A-2}$$

From this expression it is possible for any given boundary conditions $(Bi, \frac{dBi}{d\theta})$, to determine at what time (corresponding to a value of a) a given error will be exceeded. Figure A.1 gives the results for a flux ratio of E = 0.1. For given values of Bi and $\frac{dBi}{d\theta}$ a minimum value

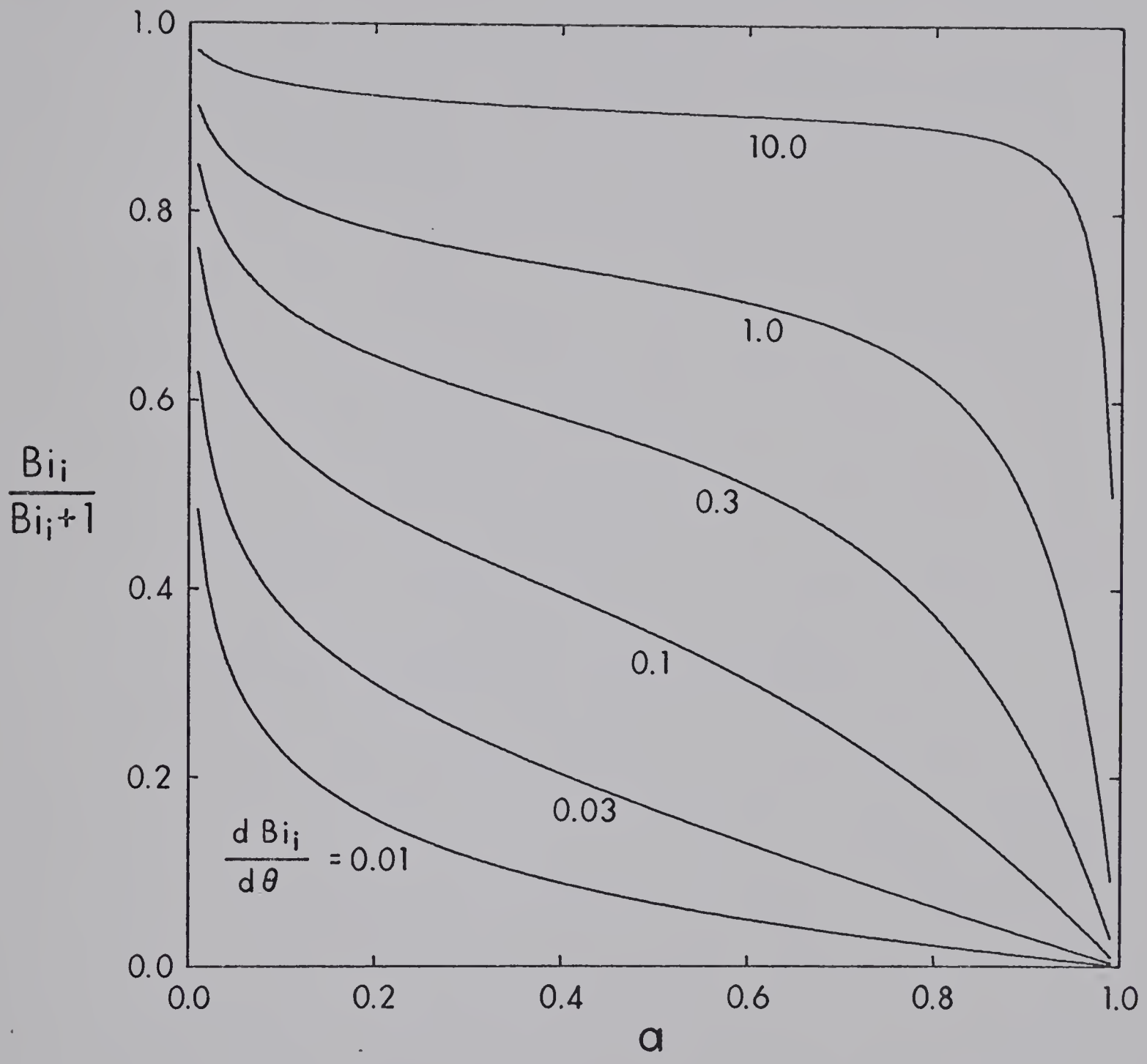

FIG. A.1: CURVES FOR E OF TEN PERCENT

of a can be found such that E is less than 0.1.

APPENDIX B

THE FULLY DEVELOPED ICE FORMATION PROFILE

APPENDIX B

THE FULLY DEVELOPED ICE FORMATION PROFILE

Figure B.1 is a plot of the results of the no-flow, no-superheat tests as given in Figure 8.1. The axes correspond to the actual physical dimensions of the test section and the ice thickness.

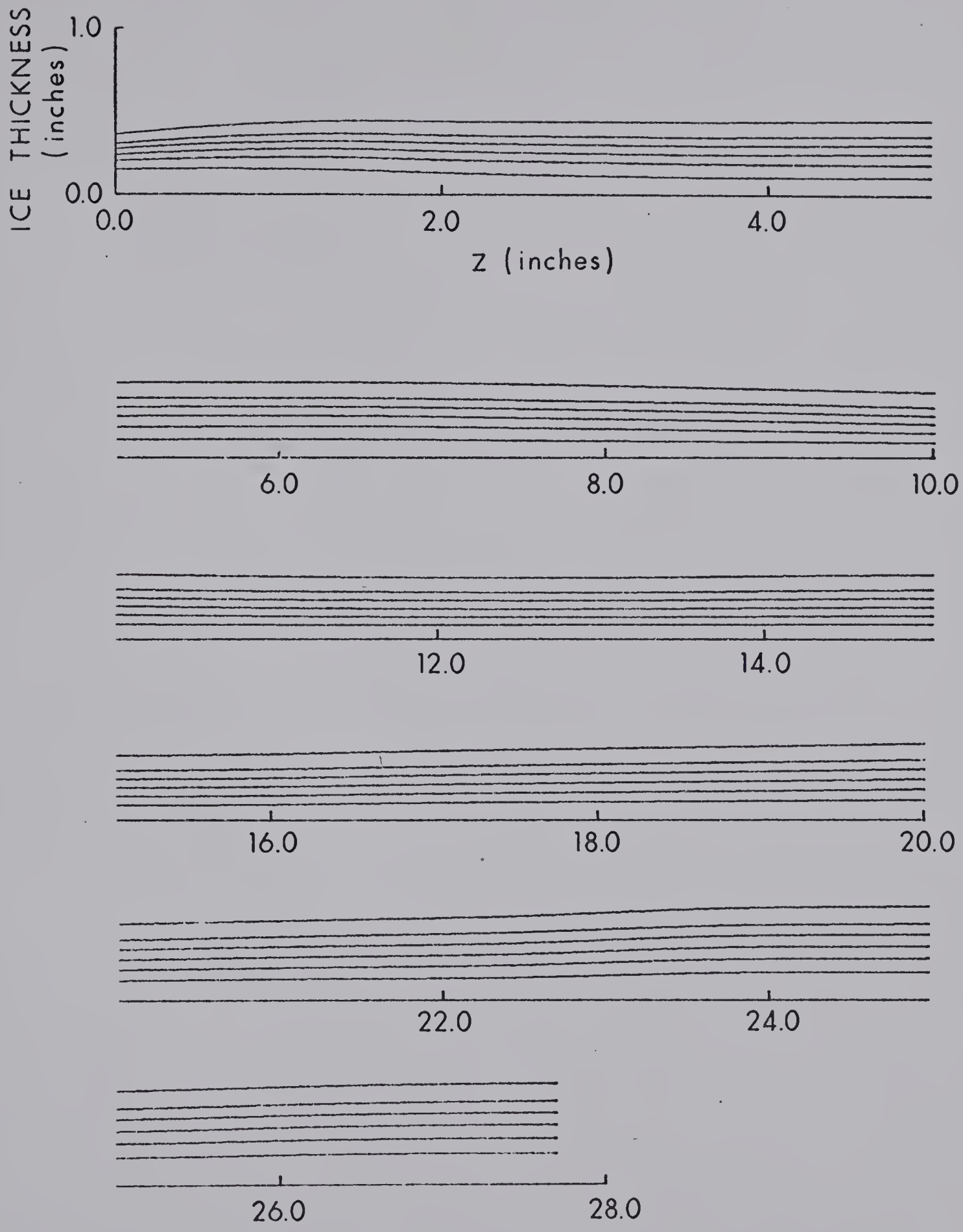

FIG. B.1: FULLY DEVELOPED ICE FORMATION